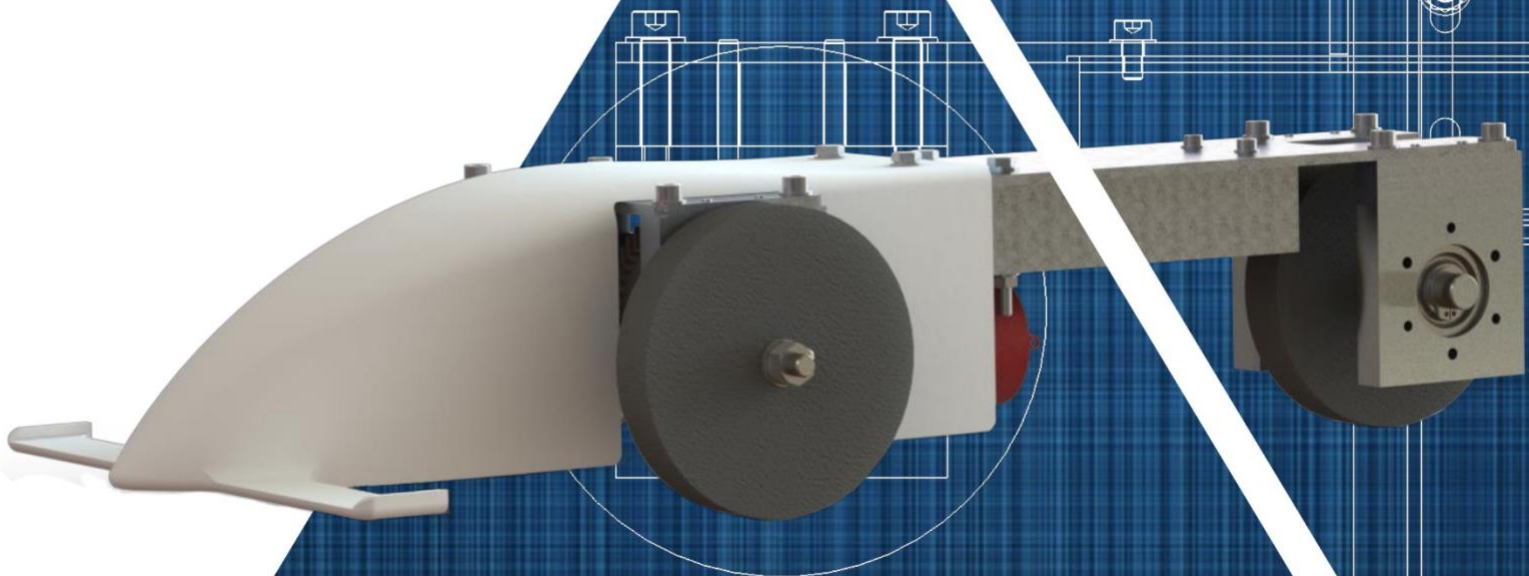


The HammerHead

Design & Manufacture
Autumn Group Project

P 2 6

Alexander Kruse
Darciea Arulnesan
Julie Leclercq
Shiva DO Kannan
Xue Xian Lim



Executive Summary

The aim of this project is to design the fastest possible miniature motorised car to compete in a race. Throughout the past 12 weeks, our team worked hard to design the HammerHead (Fig 1), following a systematic process to bring the car from the ideation stage to the technical realisation stage.

Our team created a Product Design Specification (PDS) and developed our ideas via morphological analysis. We then evaluated and ranked the design concepts using a comparison matrix. After selecting a concept, our team utilised engineering principles to design the mechanical transmission elements and the structural elements to maximise the speed of the car without compromising on safety and durability.

The resultant prototype is a front-wheel drive car with 3 wheels arranged in a tadpole configuration and a straight bevel gear transmission with a 1:3 gear ratio. An additively manufactured cover shields the transmission elements while guiding the car along the side walls of the track. Despite only weighing 1.8 kg and measuring 514 x 198 x 73 mm, The Hammerhead is able to comfortably withstand a 76 kg distributed load. The HammerHead is predicted to complete the 25 m track in 6.99 s and reach a top speed of 5.24 m s^{-1} during the race.

Additionally, our team was also tasked to tailor our prototype design for a client who wishes to manufacture approximately 1000 environmentally responsible toy cars. The car's design was simplified while the electric motor was replaced with a friction motor. Moreover, in line with the theme of environmental friendliness, the car would be made of sustainably sourced bamboo and recycled aluminium using energy-efficient manufacturing processes.

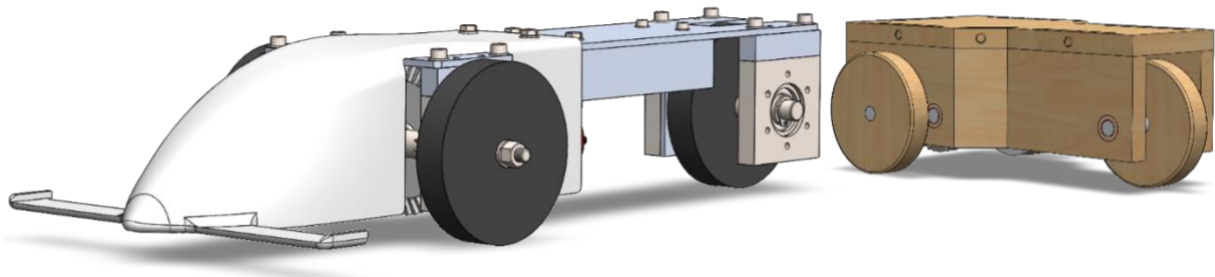


Figure 1: Prototype for Racing (Left) and Environmental Friendliness (Right)

Table of Contents

Executive Summary	2
Introduction.....	3
Design Justification	3
Design Conceptualisation.....	3
Design Embodiment.....	6
Technical Realisation	11
Proposal for Manufacture.....	17
Conclusion	23
References.....	24
Appendices.....	25

Introduction

In the autumn of 2020, Dr Marc Masen tasked 32 ME2 teams to design from scratch a miniature motorised car to compete in a race at the end of the summer term in 2021. The exciting race is slated to take place right within the home of the Mechanical Engineering department itself – on a straight track in the City and Guilds Building concourse spanning approximately 25 m. This project drew upon all our design and engineering knowledge learnt thus far and this report documents our team's process of designing the HammerHead, which we believe will be a serious contender for the race.

While the primary purpose of the car was to race, the brief also set out several other functional requirements for the car in terms of safety and durability. As with most other projects, budget, material and resource constraints were imposed as well. Nevertheless, beyond these requirements, the open-ended nature of the brief allowed for a great degree of freedom in design. Approaching such an open-ended task meant that our team had to adopt a structured design process to narrow down the possibilities and subsequently, select a design concept and continuously refine it to best satisfy the task requirements.

Our design process is expounded upon in three sections: Design Conceptualisation, Design Embodiment and Technical Realisation. The first section describes the conceptualisation and selection of our design concept. The next section details the evolution of our design concept through the major design decisions made by our team. The following section consists of the assembly drawings and a selection of detail drawings which showcase the technical details of our design.

Our team was also given an auxiliary task to adapt the design for a company with a focus on environmental sustainability. The final section of our report – Proposal for Manufacture – details the modifications made to our prototype, with emphasis on the choice of materials and manufacturing processes to best suit the client's requirements for a commercially-viable yet environmentally-responsible toy car.

Design Justification

Design Conceptualisation

Our team followed a structured and logical design process to develop design concepts for the car.

Product Design Specification

Firstly, we analysed the project brief and translated its various requirements into a PDS (Table 1).

Table 1: Product Design Specification

Category	Elements	Statement/Criteria	Verification
<i>Operation</i>	Speed	Complete an approximately 25 m long straight track in the shortest time possible. This requires the best trade-off between acceleration and top speed.	Prototype Test
	Size	Maximum width of 200 mm, no length or height restrictions. Cover restricted to a maximum base size of 254 x 254 mm and a maximum height of 305 mm.	Design Review
	Weight	Optimal weight for performance. Too light and there might not be sufficient traction. Too heavy and the car will be sluggish.	Analysis and Calculations
	Ease of Usage	On-off switch must be accessible when car is on the floor on its wheels, without removing parts or lifting the car.	Design Review
	Environment	Car will be tested in a controlled environment at the City and Guilds Building concourse. Surface is flat and relatively smooth. The track will be flanked by wooden planks about 1 inch high.	N/A
<i>Life</i>	Service Life	Last for at least 100 h of operation.	Analysis and Calculations
	Maintenance	Maintenance-free.	Design Review
<i>Production</i>	Manufacturing Time	Maximum of 12 manufacturing hours in the STW.	STW Production Plan

<p>2</p>	<ul style="list-style-type: none"> - Bevel gears - T-shaped chassis - 3 Ø 50 mm wheels - Transmission elements housed within a top plate, a bottom plate and 2 side plates - Teardrop-shaped cover 	<ul style="list-style-type: none"> - Fragile transmission elements protected by a durable box frame - Simple transmission - Aerodynamic and compact design 	<ul style="list-style-type: none"> - Needs a lot of fasteners to secure all the plates together - 3-wheel design might be unstable
<p>3</p>	<ul style="list-style-type: none"> - Spur gears - Narrow platform chassis - 3 wheels - Motor offset to one side and balanced by counterweights on other side - Airplane-shaped cover 	<ul style="list-style-type: none"> - Simple transmission - Easy to manufacture - Compact design 	<ul style="list-style-type: none"> - Counterweights add extra weight to the car - 3-wheel design might be unstable
<p>4</p>	<ul style="list-style-type: none"> - Spur and bevel gears - Low platform chassis with 2 side walls - 4 wheels - 4-wheel drive - Cambered cover sits on top of side walls 	<ul style="list-style-type: none"> - 4-wheel drive theoretically gives more grip - Low centre of gravity and wide profile provides stability 	<ul style="list-style-type: none"> - Many transmission components which add extra weight and complexity
<p>5</p>	<ul style="list-style-type: none"> - Spur gears - T-shaped chassis with components mounted on top - 3 wheels - Teardrop-shaped cover 	<ul style="list-style-type: none"> - Lightweight - Simple transmission - Easy to manufacture - Aerodynamic and compact design 	<ul style="list-style-type: none"> - Might be too fragile - 3-wheel design might be unstable

Concept Evaluation and Selection

As the preferences of each team member were highly subjective, our team utilised a comparison matrix (Table 4) to evaluate the viability and effectiveness of each design fairly and objectively. The criteria were referenced from the PDS and their relative importance were collectively agreed upon. As can be seen, our team placed greater emphasis on the effectiveness of power transmission, weight, durability and reliability.

After thorough consideration and justification, our team chose design 2 which scored highly in the important criteria. Straight bevel gears have an efficiency of 93 – 97% (Childs, 2019) so the design's simple, single-stage transmission means that power will be effectively transmitted from the motor to the main shaft directly without the need for additional shafts in between. The frame that protects the transmission elements has a high second moment of area and can withstand heavy loads while still remaining relatively light as it is hollow. The small Ø 50 mm wheels have a moment of inertia that is only 15% that of Ø 80 mm wheels and 35% that of Ø 65 mm wheels. Using **3 wheels** saves the weight of 1 wheel and allows the rear of the car to be made with less material, thus reducing weight further.

Table 4: Comparison Matrix for Ranking of Designs

Criteria	Weight	Power Transmission	Cost	Size	Manufacturing Time	Durability	Reliability	Aesthetics	Total	Weightage
Weight		0	1	1	1	0	1	1	5	0.179
Power Transmission	1		1	1	1	1	1	1	7	0.250
Cost	0	0		0	1	0	0	1	2	0.0714
Size	0	0	1		1	0	0	1	3	0.107
Manufacturing Time	0	0	0	0		0	0	1	1	0.0357
Durability	1	0	1	1	1		0	1	5	0.179
Reliability	0	0	1	1	1	1		1	5	0.179
Aesthetics	0	0	0	0	0	0	0		0	0

Note that a 1 indicates that the criterion in the row is relatively more important than the criterion in the column.

The main limitation of design 2 was the instability of the 3-wheel design. However, given that the track was straight, and no turning was involved, this was an inconsequential concern. Furthermore, the front-wheel drive meant that most of the components were near the main shaft and the centre of gravity would therefore be closer to the front where the 2 wheels were. These factors render it highly unlikely that the car would tip over to the left or right. It was also argued that a 3-wheel car might be more likely to veer away from a straight path. However, the counterargument was that a 3-wheel car could travel just as straight as a 4-wheel car if its axles were aligned properly. In addition, it was noted that the cover of the car could be designed to utilise the wooden planks at the side of the track to guide its path.

Design Embodiment

Having chosen a design concept, our team was ready to design the various components of the car in detail. Given that the performance of the car was contingent on the moving mechanical components of the car such as the gears, bearings, and shafts, these had to be chosen and designed first. The rest of the structural components could then be developed to accommodate these critical components.

Drive Transmission

The first and most crucial stage of the design embodiment was to determine the ideal gear ratio as this would directly affect the acceleration and the top speed of the car. A high gear ratio translates to an increase in torque but a reduction in speed of the main shaft, meaning that the car accelerates faster but has a lower top speed. A low gear ratio has the opposite effect, meaning that the car accelerates slower, but has a higher top speed. A balance needs to be struck between the two variables to minimise the time taken for the car to complete the race.

We used the motor torque-speed characteristic curve to calculate how the torque varied on the main shaft as its speed varied. This torque provides the driving force that the wheels exert on the ground to propel the car forward. Thus, using Newton's second law, we were able to relate this force to the acceleration of the car and subsequently solve the differential equation to obtain the car's speed as a function of time. Further integration and differentiation yielded the car's distance and acceleration as a function of time. Detailed calculations are shown in Appendix A.

A Python code was implemented to plot the functions. The code iteratively solved the equations for various gear ratios to determine the ideal gear ratio that would give the minimum time taken to complete the race. It showed that the minimum time of 6.99 s is achieved with a **gear ratio of 1:3** (Fig 2). The car is predicted to reach a speed of 5.24 m s^{-1} when crossing the finish line.

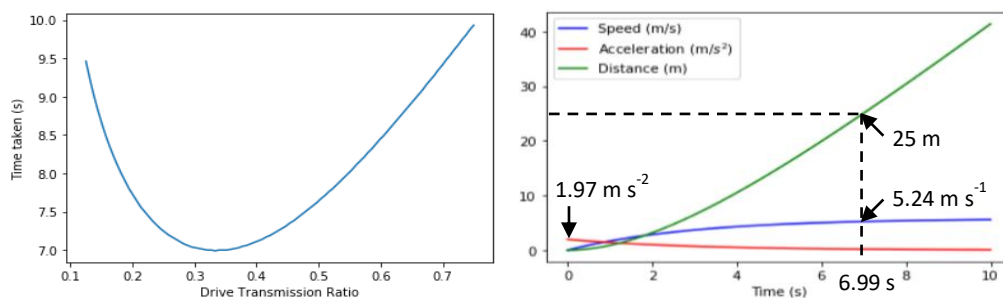


Figure 2: Time Taken to Travel 25 m for Different Gear Ratios (Left) and Distance, Speed and Acceleration Plots for a 1:3 Gear Ratio (Right)

With this data, we could now select the gears. **Bevel gears** were chosen over spur gears since a bevel gear arrangement would allow the motor to be aligned along the centre axis of the car to minimise any mass imbalance that could cause the car to veer from a straight path (Fig 3). Hence, we needed to choose a set of bevel gears where the larger gear on the motor shaft would have 3 times as many teeth as the pinion gear on the main shaft.

Our team had dimensional constraints to consider when choosing a specific set of gears. While it was preferable to choose the smallest set of gears to keep the car compact and lightweight, this was limited by the hub diameter of the smaller gear that would be fitted on the supplied $\varnothing 14$ mm main shaft. If we chose a gear with a hub diameter of less than 14 mm, we would have to turn the shaft to reduce its diameter while expanding the pilot bore of the gear. This would weaken both the shaft and the gear, especially if much material were to be removed. Hence, it was ideal to choose a gear with a hub diameter larger than 14 mm.

Taken to the other extreme, we could have chosen a very large set of gears to solve the above constraint. However, as aforementioned, this would result in a larger and heavier car. Moreover, the gear would come into contact with the chassis or the floor if its diameter was too large.

Since weight was a key performance parameter and the load on the gears was relatively small, our team decided that gears made of Delrin were sufficient for our needs. We chose straight bevel gears over spiral ones as our calculated pitch line velocity of 1.474 m s^{-1} (Appendix C) was well within the range of $0 - 5 \text{ m s}^{-1}$ that straight bevel gears are recommended for (Childs, 2019). We concluded that the **15 and 45-toothed GCZTB1.5 bevel gear set** best suited our needs.

To confirm our choice of gears, our team checked that they could withstand the bending and contact stresses. A stress cycle factor for 100 h of operation was applied to the equations. The bending and contact stresses were calculated to be 3.54 MPa and 20.4 MPa respectively. These were far below their corresponding maximum permissible values of 24.0 MPa and 87.2 MPa (Appendix C). Hence, the chosen bevel gear set is sufficiently strong and will not fail due to wear before 100 h of operation.

Having chosen the gears, modifications to the initial concept design were made to accommodate them. Although we had planned to use the smallest wheels available, the larger gear in the bevel gear set had a tip diameter of 68.44 mm, necessitating the use of **$\varnothing 80$ mm wheels** so that the gear would not contact the floor. In addition, to accommodate the difference in diameter between the $\varnothing 15$ mm pilot bore of the large gear and the $\varnothing 5.98$ mm shaft of the motor, a reduction bushing with a set screw was required (Fig 4). To ensure that the torque of the motor shaft was effectively transmitted to the reduction bushing and to prevent the reduction bushing from slipping off the motor shaft, the bore of the reduction bushing was tightly toleranced for an interference fit. A transition fit was applied to the outer diameter of the reduction bushing and the bore of the gear. A set screw was also used to securely constrain the gear and reduction bushing both radially and axially.

Bearings

Deep groove ball bearings were chosen to reduce friction and to accommodate the radial and axial loads of the drive transmission. The supplied bearing housings already had a $\varnothing 26$ mm bore with a H7 tolerance while the supplied shafts had $\varnothing 10$ mm sections on either end with a j6 tolerance. It was thus practical and sensible for our team to use bearings with 26 mm OD and 10 mm ID. Minimal modifications would then be needed to the supplied components, enabling us to keep within budget and manufacturing constraints. Our team chose the **SKF 6000-2Z** for all four bearings. These bearings are relatively cheap and have dust shields that aid longevity. They are maintenance-free and do not require relubrication during their lifetime (SKF, 2011).

We calculated the minimum required dynamic load rating to be 2.82 kN for a 10% probability of failure after 100 hours of operation. This was done using a L_{10} basic life rating of 7.51×10^6 revolutions (Appendix D). Our bearings'

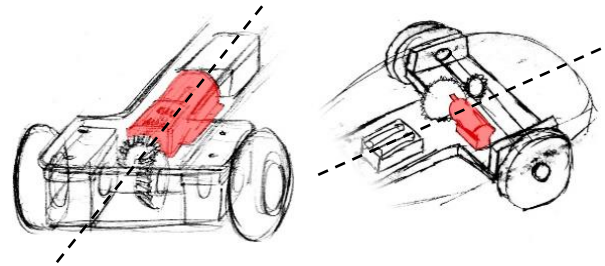


Figure 3: Centralised Motor with Bevel Gears (Left) and Offset Motor with Spur Gears (Right)

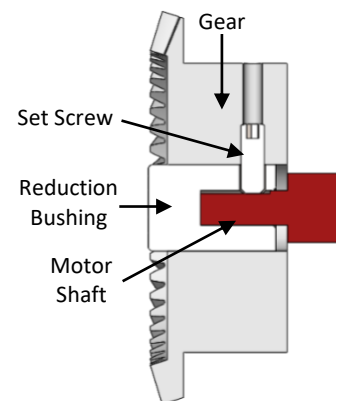


Figure 4: Section View of Motor Shaft Bevel Gear

dynamic load rating of 4.75 kN is well above the minimum required. Therefore, the possibility of a bearing failing within 100 hours of operation is remote.

Main Shaft

The main shaft needed to fulfil three requirements. Firstly, the torque needed to be transmitted effectively from the drive transmission to the wheels. This required axial and/or radial constraints on the components fitted onto the shaft. Specifically, the bearings needed to be axially constrained, whereas the bevel gear and the wheels needed to be both axially and radially constrained (Fig 5). Secondly, the shaft had to be able to withstand the weight of an average person. Thirdly, it should last for at least 100 hours of operation.

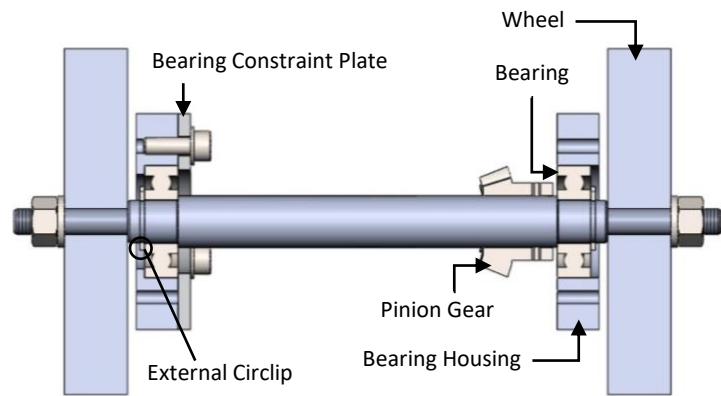


Figure 5: Main Shaft Subassembly

As the main shaft was a mandatory supplied component, our team modified it to suit our needs. The bevel gear on the shaft had a \varnothing 10 mm pilot bore while the supplied shaft had a 14 mm diameter. To not weaken the gear excessively or interfere with its teeth, it is good practice to have a bore size no larger than 70% of the hub diameter (QTC Gears, 2021) which in our case, for a \varnothing 18 mm hub, corresponded to a maximum diameter of 12.6 mm. At the same time, we could not simply turn the shaft down to \varnothing 10 mm as the bearings needed a minimum abutment diameter of 12 mm. Therefore, we chose a **diameter of 12 mm for the middle section** of the main shaft.

Our team was cautious about excessively reducing the diameter of the other sections of the shaft as well to preclude the shaft being unable to withstand the weight of a person. However, to reduce weight, we **shortened the length of the shaft from 200 mm to 168 mm**. The shaft only needed to be as long as necessary for all the components to fit on it. Any excess length was effectively dead weight and would also require a wider chassis. This method was in fact advantageous because decreasing the length reduces the maximum bending moment and increases the load that the shaft can carry. On the contrary, decreasing the diameter reduces the second moment of area and increases the stress on the shaft.

We approximated the shaft as a simply supported beam with point loads at the wheels and bearings to plot the shear force and bending moment diagrams (Fig 6). The total force acting on the shaft was rounded up to 800 N as this roughly corresponded to the average weight of a person together with the estimated weight of the car (Appendix B).

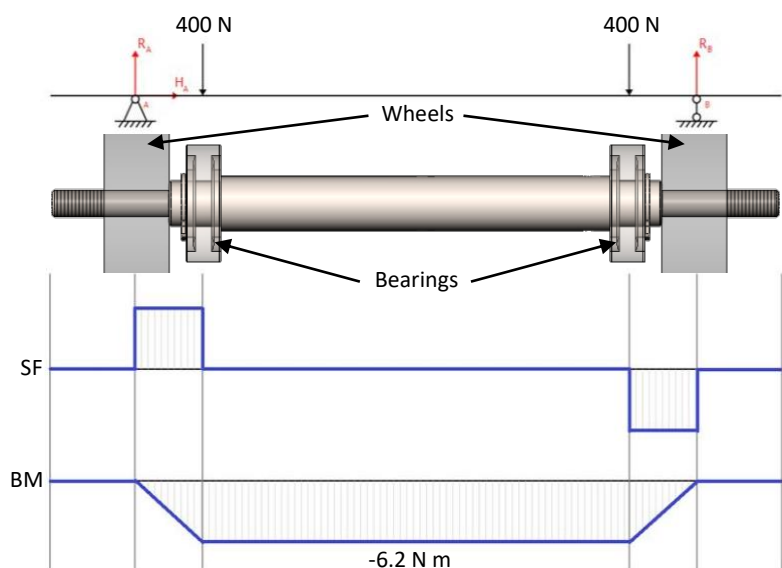


Figure 6: Stress Analysis of Main Shaft

The maximum bending moment was found to be -6.2 N m . The maximum stress in the main shaft caused by this bending moment was computed to be 63.1 MPa (Appendix E). The yield stress of EN1A mild steel is $240 - 400 \text{ MPa}$ (KV Steel Services, 2021). This would mean that the main shaft has a minimum safety factor of 3.8, making the main shaft very unlikely to yield from the stresses applied. Moreover, the main shaft operates well below its fatigue limit, with a generous safety factor of 48.2. Our team therefore concluded that the shaft would undoubtedly operate for 100 hours (Appendix E).

Rear Shaft

The purpose of the freely rotating rear shaft is to hold the single rear wheel in a properly aligned position. Misalignment of the wheel would cause the car to continuously drift to one side which would severely impact its speed. The rear wheel was constrained in the centre of the shaft with a shoulder on one side and a nut and washer on the other side (Fig 7).

To reduce cost, our team modified the supplied idler shaft rather than creating a brand-new custom component. Similar to the main shaft, while it was important to make the rear shaft light by removing as much excess material as possible, the shaft also needed to be strong enough to withstand the weight of an average person. We adopted the same strategy by conservatively removing 2 mm from the 14 mm diameter of the rear shaft while **cutting down its overall length by more than one-third**. This allowed our team to reduce the shaft's weight by more than half. The bending moment in the middle of our shaft was -11.4 N m when a person's weight was on the car (Fig 8). This gave a stress of 67.2 MPa (Appendix E). Thus, a rear shaft made of EN1A steel gives a safety factor of 3.6 proving that it is sufficiently strong.

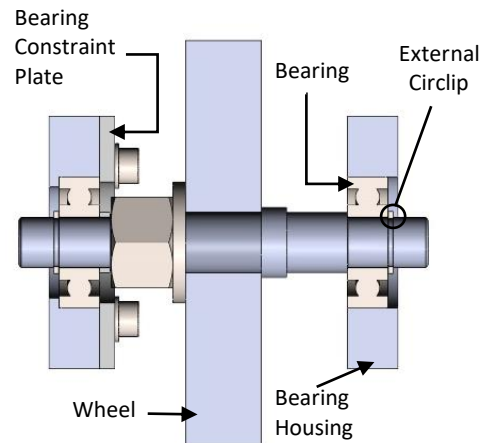


Figure 7: Rear Shaft Subassembly

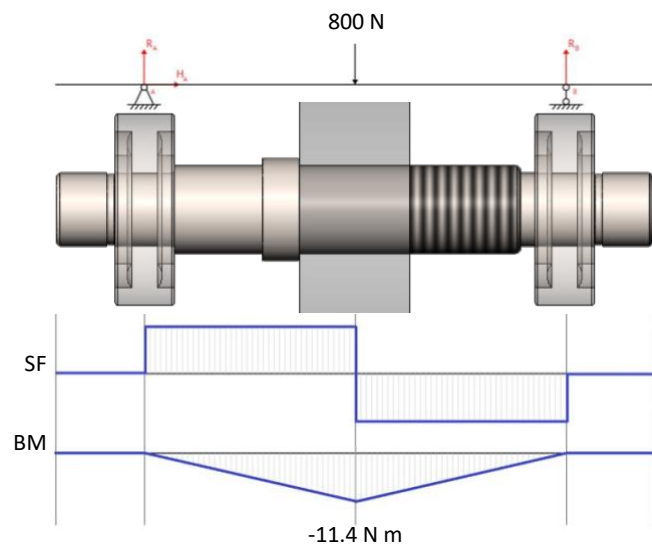


Figure 8: Stress Analysis of Rear Shaft

The bearings for the main shaft and the rear shaft are constrained in the same manner as shown in Figures 5 and 7. The inner race of all bearings are constrained on both sides with shoulders and external circlips. The outer race of one bearing on each shaft is constrained with the bearing housing shoulder and a bearing constraint plate while that of the other bearing is left floating. Thus, the bearings are accurately constrained.

Chassis

The chassis serves two significant purposes. Firstly, it holds all the components in their correct, tolerated positions. This ensures alignment of the main and rear shafts as well as proper meshing of the gears. Secondly, it supports the weight of all the components as well as any unexpected loads on the car, such as a person stepping on it.

The chassis in the initial design concept involved a frame which enclosed the transmission elements consisting of a top plate, a bottom plate, and two side plates (Fig 9). The box-like cross-section would have a high second moment of area to withstand large loads. However, unless the side plates were of a sufficient thickness to insert screws and pins, additional brackets would have been needed to secure all the plates together. Making the plates sufficiently thick to accommodate screws and pins would have added significant weight to the car while using additional brackets would have incurred steep costs.

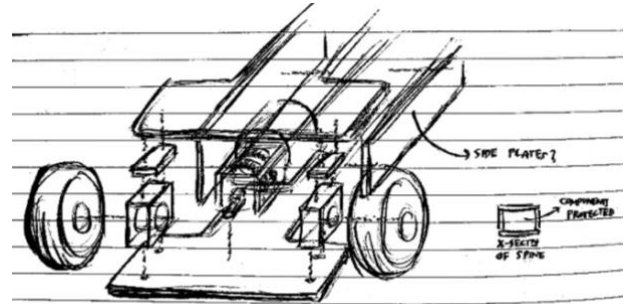


Figure 9: Initial Chassis Design Concept

After examining the list of stock materials, our team realised that there were aluminium bars with a box cross-section, similar to our original design. While not large enough to fit the transmission elements inside, these bars could still provide a high strength and stiffness to the chassis by forming the **“backbone” of the car** (Fig 10). Their hollow nature ensured the car remained relatively lightweight. The bottom and side plates were removed, as firstly, they were no longer needed as load-bearing components and secondly, it was highly unlikely that the car would be stepped on from the bottom or the sides. The motor could then be mounted upside-down on the box bars. In doing so, the bars simultaneously provided additional clearance between the motor shaft and the top plate, allowing larger gears to be fitted on the motor shaft. As the accurate positioning of transmission components was crucial for proper meshing of the bevel gears, a slight recess was milled into the top plate to position the box bars within tight tolerance. Another recess was also milled into the box bars to restrict the lateral movement of the motor. The slots in the motor base allowed the motor to be adjusted forwards and backwards slightly, and to be locked into position by tightening the nuts once the gears were confirmed to be properly meshing.

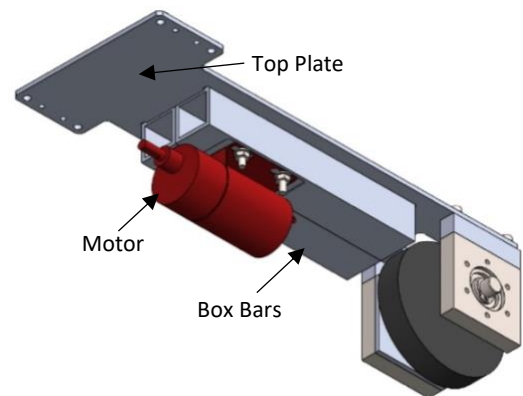


Figure 10: Inverted Motor Mounted on Box Bars

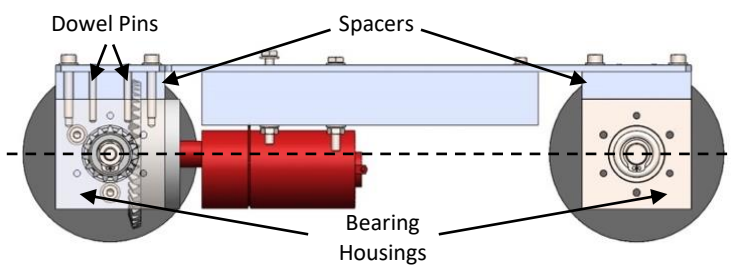


Figure 11: Proper Alignment of All Components

To align the axes of the bevel gears, and all the shafts (motor, main, and rear) on the same plane, spacers were added between the top plate and bearing housings (Fig 11). Dowel pins were used to accurately position these components. As can be seen, the chassis ensures all components are positioned correctly relative to one another within tight tolerances so that the bevel gears can effectively transmit power.

The two places on the chassis that our team postulated would be the most susceptible to yield failure, were in the middle, where the bending moment would be the highest and at the rear region, where the top plate was not reinforced by the box bars (Fig 12). Taking a conservative approach, we considered a realistic scenario, where a person placed his entire weight on a single foot at the centre of the car with their foot oriented perpendicularly to the longitudinal axis of the car. The free-body diagrams and bending moment diagrams are shown in Figure 12. The distributed load was taken to act over a length of 103 mm, which corresponded to the width of a size 10 shoe – the average shoe size of a UK male (BBC, 2014).

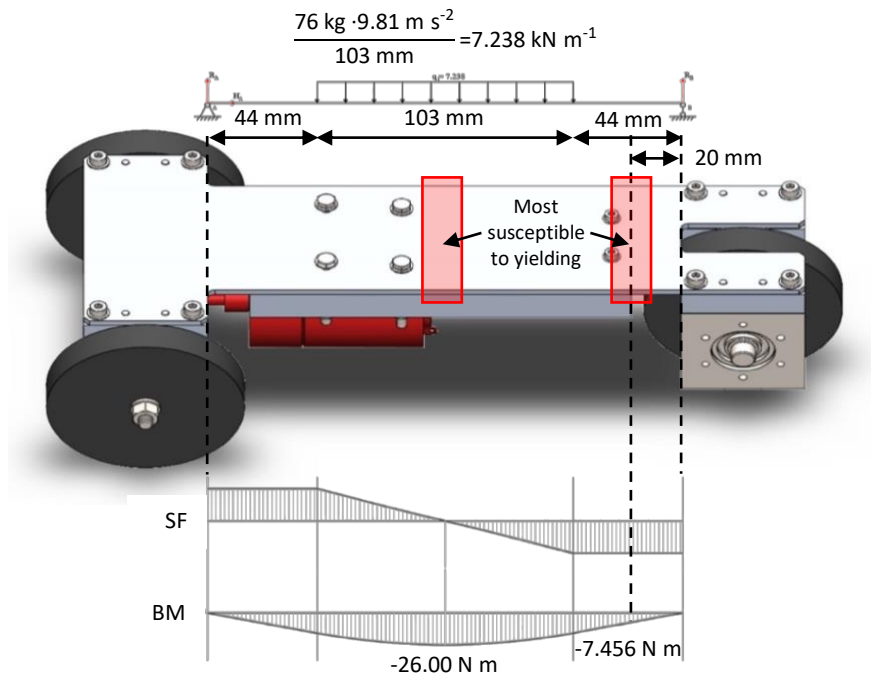


Figure 12: Stress Analysis of Chassis

The stress at the middle was calculated to be 6.58 MPa and 72.0 MPa at the rear (Appendix F). The yield strength of cast acrylic is 57.8 – 63.7 MPa while that of 6082-T6 aluminium is 240 – 280 MPa (GRANTA Edupack, 2020). Our team also noted from consultation with seniors and the STW staff that acrylic has a tendency to crack when machined. Aluminium was therefore chosen for its strength and machinability. The safety factor of 3.3 proves that the chassis is categorically able to support the weight of a person accidentally stepping on it without suffering permanent deformation.

Cover

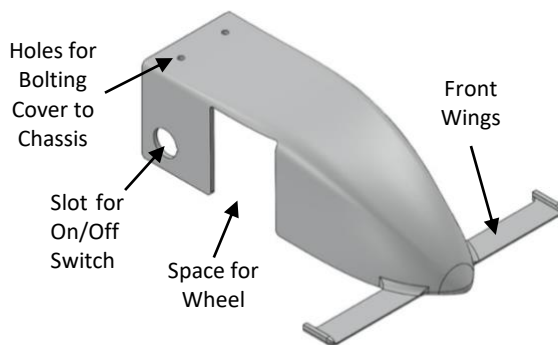


Figure 13: Additively Manufactured Cover

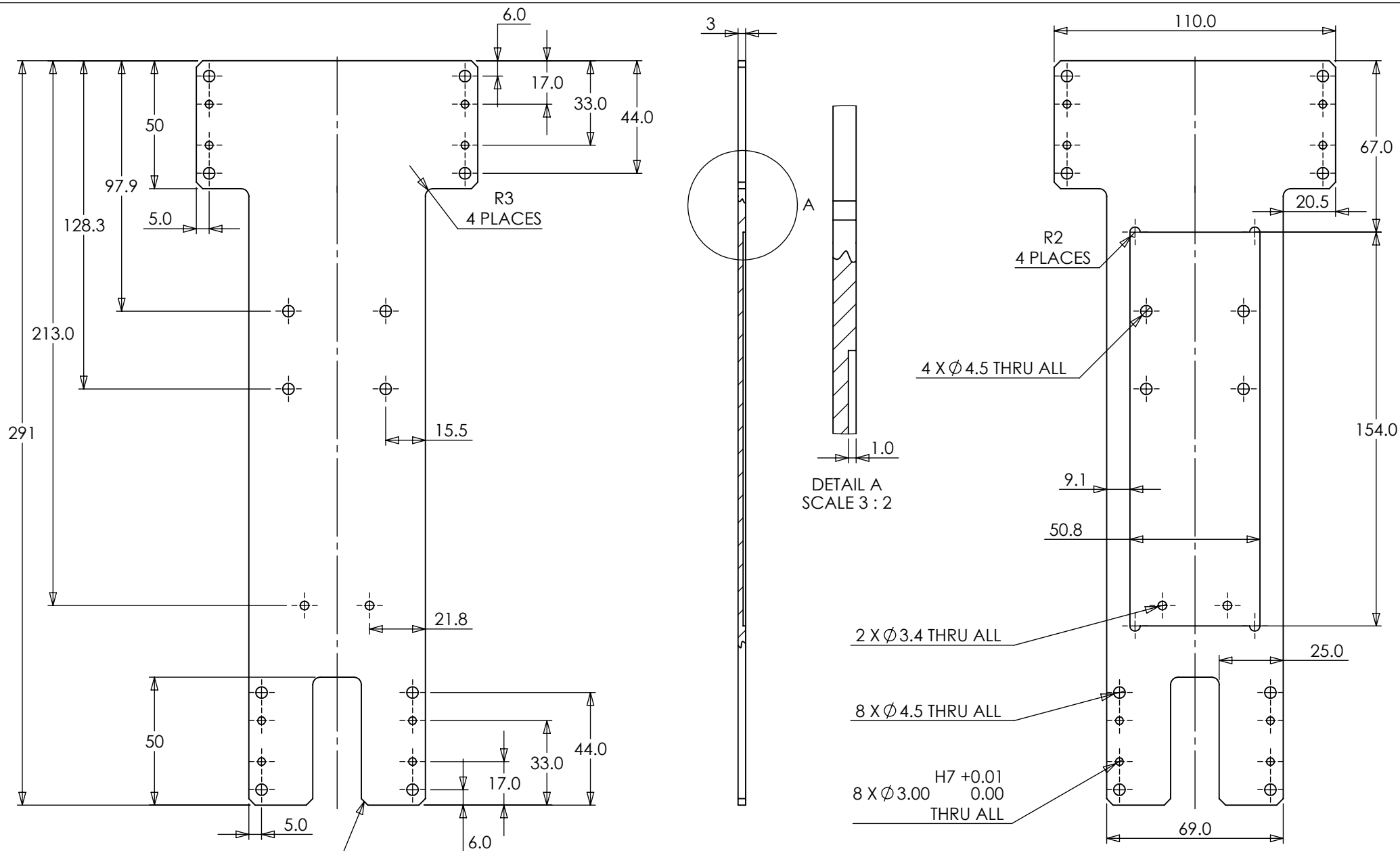
While conceptualising the 3D printed external shell of the car, our team acknowledged two requirements that the cover needed to satisfy. Firstly, the cover had to shield the transmission elements for the user's safety. Secondly, it needed to be lightweight and reasonably aerodynamic to avoid adding excessive weight and drag to the car. We also noted that the cover was not intended to be a load-bearing component and would simply sit atop the chassis.


We drew inspiration from the design of other fast-moving objects and settled on the simple design shown in Figure 13. The cover only covers the front of the HammerHead due

to the limited size of the 3D printer bed. Nevertheless, it meets the requirement of covering the transmission elements. The front wings were dimensioned to be as wide as the track to guide the car in a straight path along the side walls as we particularly did not want the rubber wheels to contact the side walls due to its high coefficient of friction. A slot was cut out on the side of the cover for snap fixing of the switch so that the switch is easily accessible.

Technical Realisation

The following section consists of a selection of engineering drawings to showcase the technical details of our design: three detail drawings, the main shaft subassembly drawing, and the general assembly drawings.

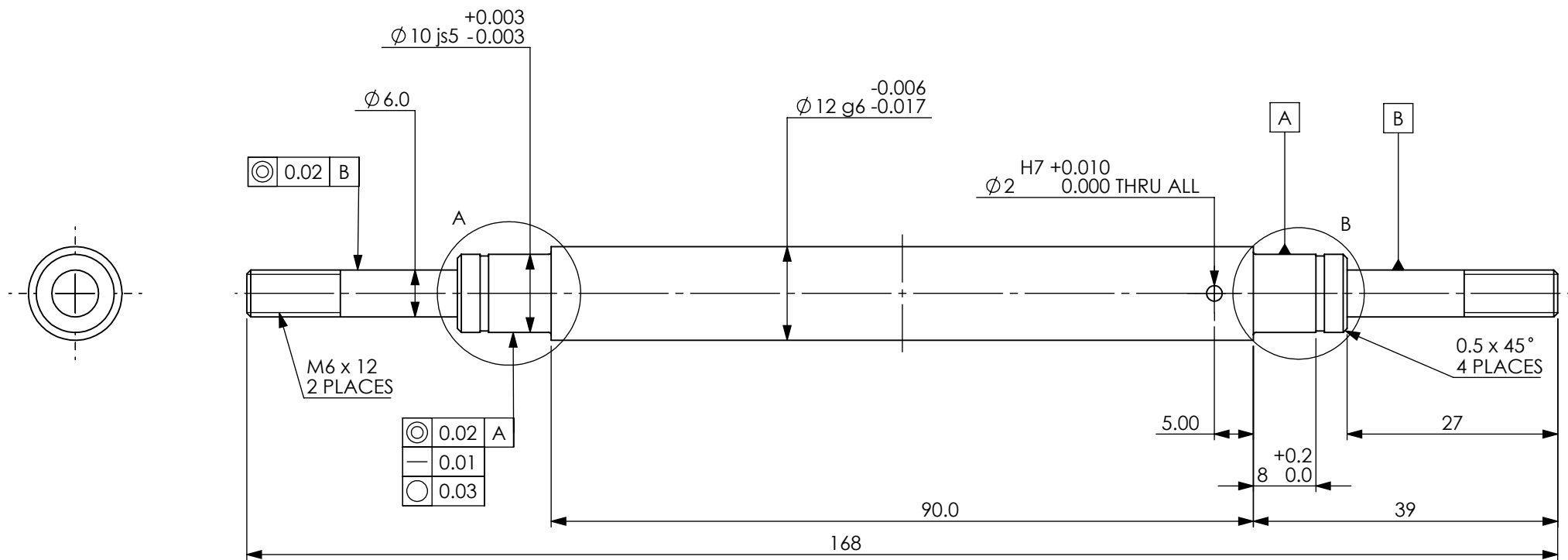


TOLERANCES		THIRD ANGLE PROJECTION
X = ± 0.5	ANGULAR ± 1°	
X.X = ± 0.1	SURFACE FINISH	
X.XX = ± 0.02	MACHINED	
	FACES Ra 6.3	
	NAME	DATE
DRAWN	X. X. LIM	03/11/20
CHECKED	A. KRUSE	04/11/20
APPROVED	D. ARULNESAN	06/11/20

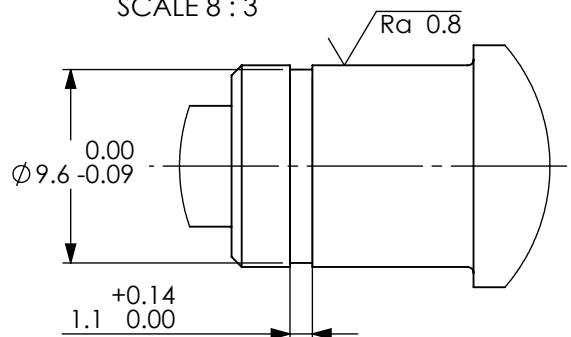
MATERIAL: ALUMINIUM 6082 T6	
ALL DIMENSIONS ARE IN MILLIMETRES	
DO NOT SCALE DRAWING	
A4	SCALE 1:2

TITLE: CHASSIS
DWG No. CAR-04

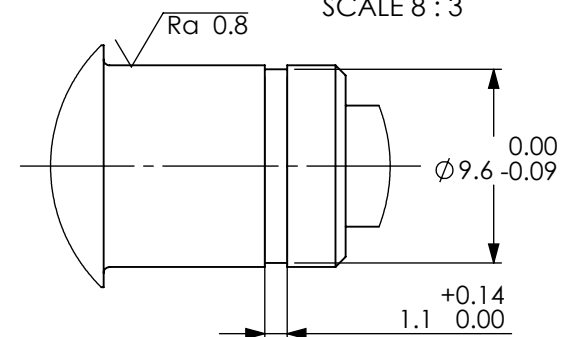
Imperial College London	
Department of Mechanical Engineering	
SHEET 1 OF 1	REVISION 3



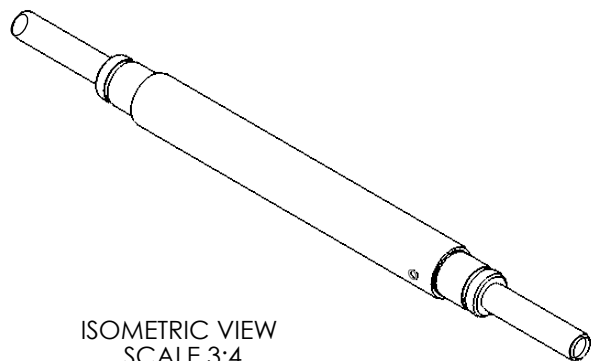
DETAIL A
SCALE 8 : 3

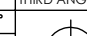


DETAIL B
SCALE 8 : 3



ISOMETRIC VIEW
SCALE 3:4

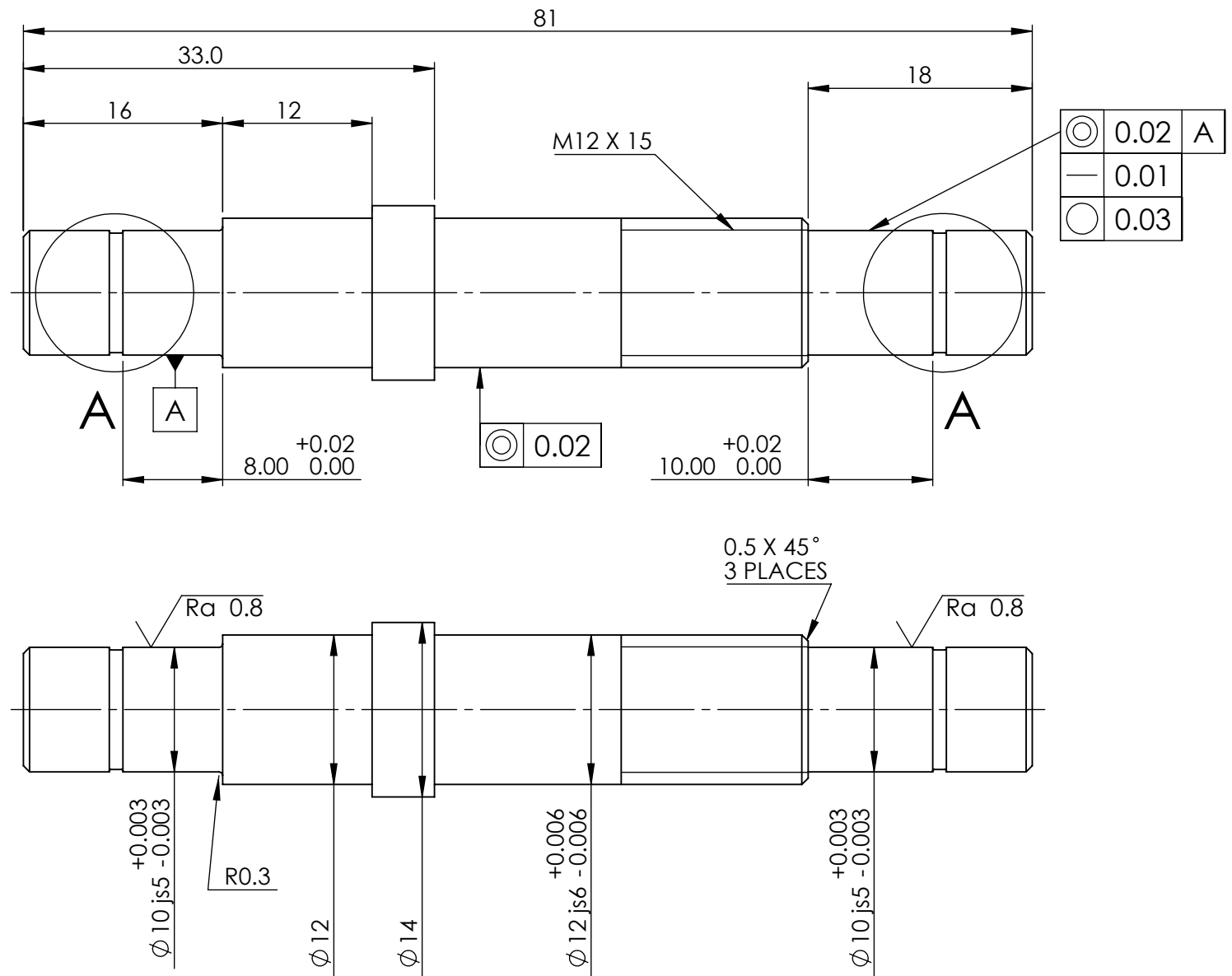



TOLERANCES		
X = ± 0.5	ANGULAR ±1°	
X.X = ± 0.1	SURFACE FINISH	
X.XX = ± 0.02	MACHINED FACES Ra 6.3	
	NAME	DATE
DRAWN	J. LECLERCQ	02/11/20
CHECKED	S. SANGEETHA	04/11/20
APPROVED	A. KRUSE	05/11/20

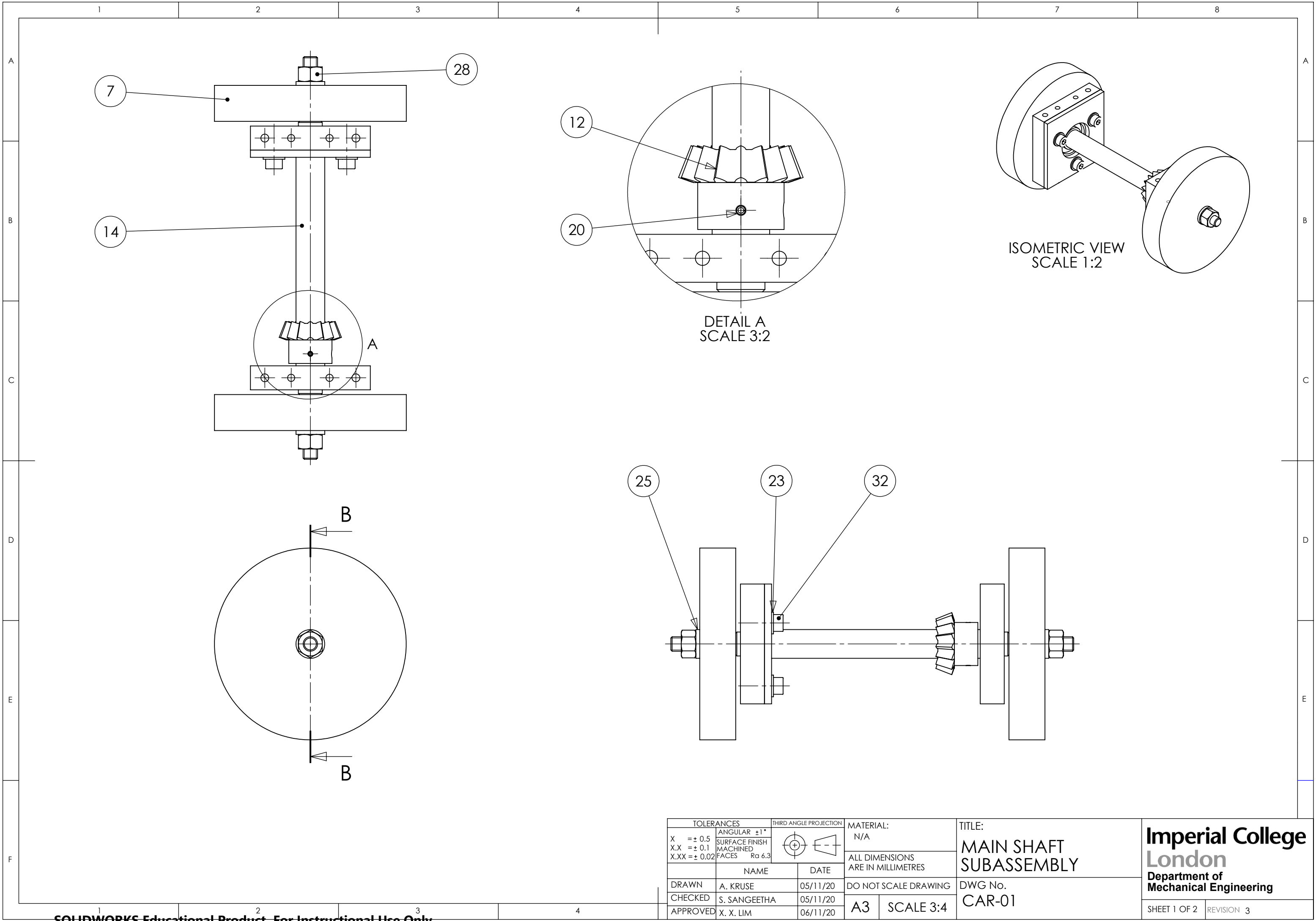
MATERIAL:		TITLE:	
MILD STEEL EN1A		MAIN SHAFT	
ALL DIMENSIONS ARE IN MILLIMETRES		DWG No.	
DO NOT SCALE DRAWING		ME2DMF-SS-01A	
A4		SCALE 4:3	

TITLE:		MAIN SHAFT	
DWG No.		ME2DMF-SS-01A	
DO NOT SCALE DRAWING		SCALE 4:3	
A4		SCALE 4:3	

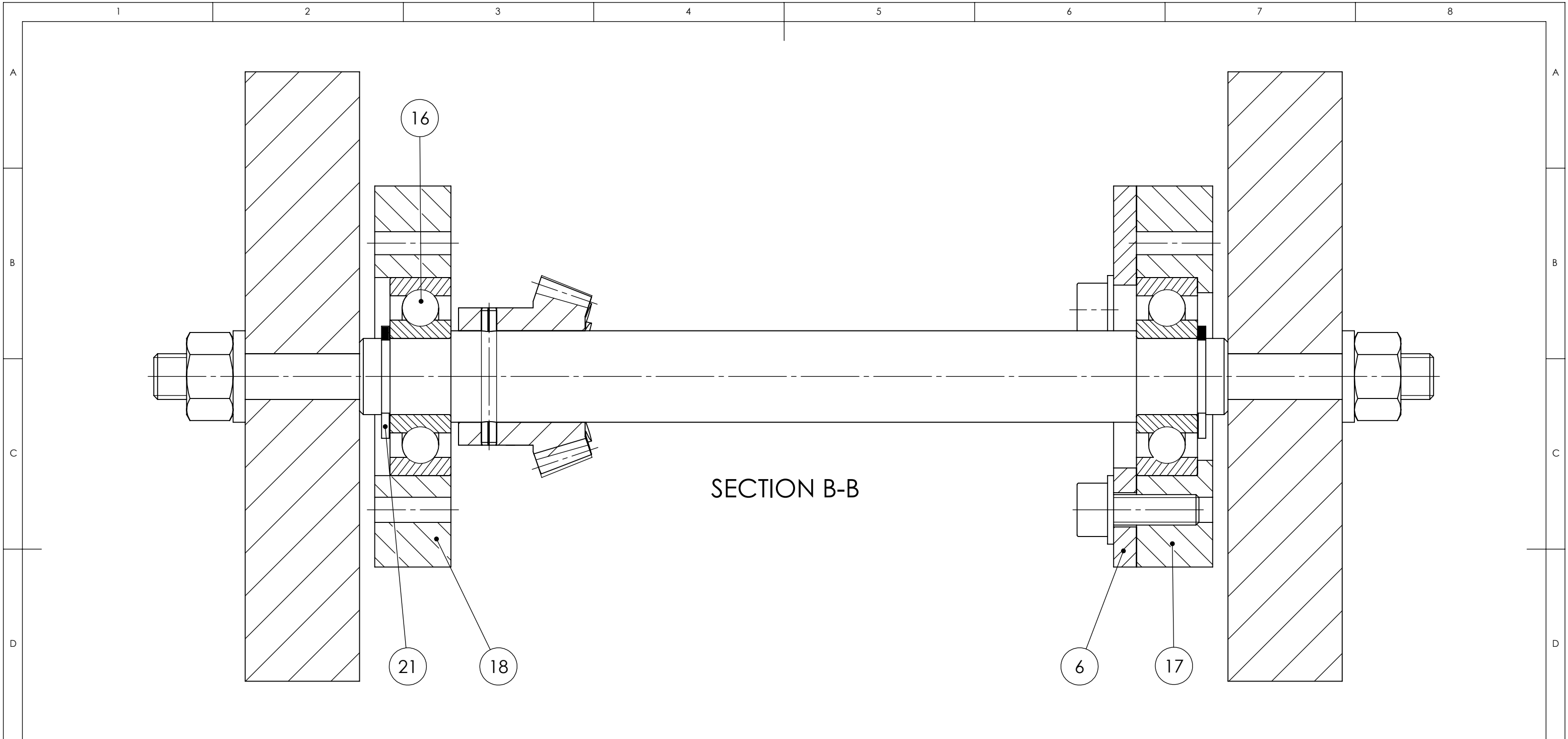
Imperial College London			
Department of Mechanical Engineering			
SHEET 1 OF 1		REVISION 3	



TOLERANCES		THIRD ANGLE PROJECTION		MATERIAL: MILD STEEL EN1A		TITLE: REAR SHAFT		<div>Imperial College London Department of Mechanical Engineering</div>		
X =± 0.5	ANGULAR ±1°									
X.X =± 0.1	SURFACE FINISH									
X.XX =± 0.02	MACHINED FACES Ra 6.3									
		NAME		DATE		ALL DIMENSIONS ARE IN MILLIMETRES				
DRAWN	D. ARULNESAN		03.11.20		DO NOT SCALE DRAWING		DWG No.			
CHECKED	A. KRUSE		04.11.20		A4 SCALE 2:1		ME2DMF-SS-02A			
APPROVED	S. SANGEETHA		05.11.20						SHEET 1 OF 1	

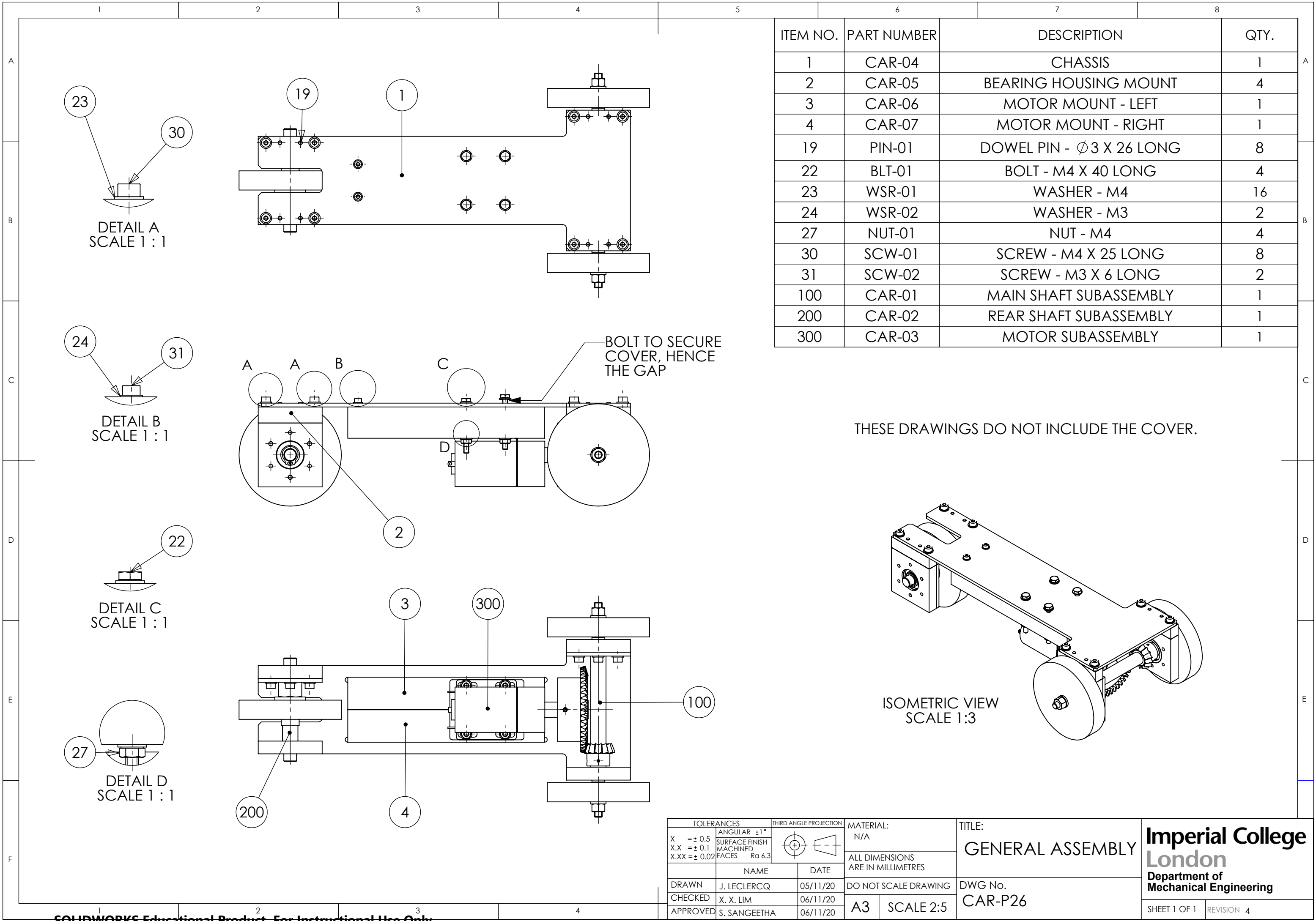


TOLERANCES		THIRD ANGLE PROJECTION		MATERIAL:		TITLE:		Imperial College London Department of Mechanical Engineering	
X	± 0.5	ANGULAR	± 1°	N/A		MAIN SHAFT SUBASSEMBLY			
X.X	± 0.1	SURFACE FINISH		ALL DIMENSIONS ARE IN MILLIMETRES				DWG No. CAR-01	
X.XX	± 0.02	MACHINED FACES Ra 6.3							
	NAME		DATE	DO NOT SCALE DRAWING				SHEET 1 OF 2 REVISION 3	
DRAWN	A. KRUSE		05/11/20						
CHECKED	S. SANGEETHA		05/11/20	A3 SCALE 3:4					
APPROVED	X. X. LIM		06/11/20						



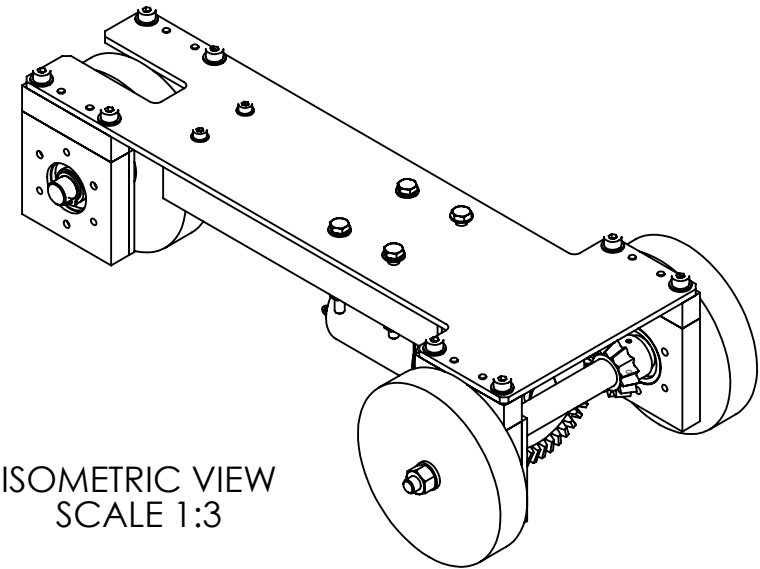
ITEM NO.	PART NUMBER	DESCRIPTION	QTY.
6	CAR-09	BEARING CONSTRAINT PLATE	1
7	CAR-10	FRONT WHEEL	2
12	GCZTB1.5-15A	BEVEL GEAR - 15T	1
14	ME2DMF_SS_01A	MAIN SHAFT	1
16	SKF 6000-2Z	BEARING - ID 10 OD 26	2
17	ME2DMF_BH_03	BEARING HOUSING	1
18	ME2DMF_BH_03A	MODIFIED BEARING HOUSING	1
20	PIN-02	SPRING PIN - $\varnothing 2$ X 18 LONG	1
21	BS 3673-4-S010M	EXTERNAL CIRCLIP - ID 10	2
23	WSR-01	WASHER - M4	3
25	WSR-03	WASHER - M6	2
28	NUT-02	NUT - M6	2
32	SCW-03	SCREW - M4 X 12 LONG	3

TOLERANCES		THIRD ANGLE PROJECTION		MATERIAL:		TITLE:		<div>Imperial College London Department of Mechanical Engineering</div>	
X	= ± 0.5	ANGULAR	± 1°	N/A		MAIN SHAFT SUBASSEMBLY			
X.X	= ± 0.1	SURFACE FINISH		ALL DIMENSIONS ARE IN MILLIMETRES		DWG No.			
X.XX	= ± 0.02	MACHINED FACES		Ra 6.3		DO NOT SCALE DRAWING		CAR-01	
DRAWN		NAME		DATE		A3		SCALE 2:1	
CHECKED		S. SANGEETHA		05/11/20					
APPROVED		X. X. LIM		06/11/20					
SHEET 2 OF 2								REVISION 3	

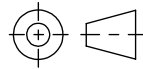


ITEM NO.	PART NUMBER	DESCRIPTION	QTY.
1	CAR-04	CHASSIS	1
2	CAR-05	BEARING HOUSING MOUNT	4
3	CAR-06	MOTOR MOUNT - LEFT	1
4	CAR-07	MOTOR MOUNT - RIGHT	1
19	PIN-01	DOWEL PIN - $\varnothing 3$ X 26 LONG	8
22	BLT-01	BOLT - M4 X 40 LONG	4
23	WSR-01	WASHER - M4	16
24	WSR-02	WASHER - M3	2
27	NUT-01	NUT - M4	4
30	SCW-01	SCREW - M4 X 25 LONG	8
31	SCW-02	SCREW - M3 X 6 LONG	2
100	CAR-01	MAIN SHAFT SUBASSEMBLY	1
200	CAR-02	REAR SHAFT SUBASSEMBLY	1
300	CAR-03	MOTOR SUBASSEMBLY	1

THESE DRAWINGS DO NOT INCLUDE THE COVER.



TOLERANCES		THIRD ANGLE PROJECTION		MATERIAL: N/A		TITLE: GENERAL ASSEMBLY		<div>Imperial College London</div> <div>Department of Mechanical Engineering</div>	
X	± 0.5			ALL DIMENSIONS ARE IN MILLIMETRES					
X.X	± 0.1								
X.XX	± 0.02								
		NAME		DATE		DWG No. CAR-P26			
DRAWN	J. LECLERCQ		05/11/20						
CHECKED	X. X. LIM		06/11/20						
APPROVED	S. SANGEETHA		06/11/20						
				A3	SCALE 2:5			SHEET 1 OF 1	
								REVISION 4	

1		2		3		4		5		6		7		8	
ITEM NO.		PART NUMBER		DESCRIPTION		MATERIAL		QTY.		SUBASSEMBLY DWG NO.					
A	1	CAR-04		CHASSIS		ALUMINIUM 6082 T6		1		CAR-P26					
	2	CAR-05		BEARING HOUSING MOUNT		ALUMINIUM 6082 T6		4		CAR-P26					
	3	CAR-06		MOTOR MOUNT - LEFT		MILD STEEL EN1A		1		CAR-P26					
	4	CAR-07		MOTOR MOUNT - RIGHT		MILD STEEL EN1A		1		CAR-P26					
B	5	CAR-08		COVER		ABS PLASTIC		1		CAR-P26					
	6	CAR-09		BEARING CONSTRAINT PLATE		ALUMINIUM 6082 T6		2		CAR-01, CAR-02					
	7	CAR-10		FRONT WHEEL		SILICONE RUBBER SHORE HARDNESS 60A		2		CAR-01					
	8	CAR-11		REAR WHEEL		SILICONE RUBBER SHORE HARDNESS 60A		1		CAR-02					
C	9	CAR-12		SPACER		MILD STEEL EN1A		1		CAR-02					
	10	CAR-13		MOTOR		N/A		1		CAR-03					
	11	CAR-14		REDUCTION BUSHING		MILD STEEL EN1A		1		CAR-03					
	12	GCZTB1.5-15A		BEVEL GEAR - 15T		POLYOXYMETHYLENE (DELRIN)		1		CAR-01					
D	13	GCZTB1.5-45		BEVEL GEAR - 45T		POLYOXYMETHYLENE (DELRIN)		1		CAR-03					
	14	ME2DMF_SS_01A		MAIN SHAFT		MILD STEEL EN1A		1		CAR-01					
	15	ME2DMF_SS_S_01A		REAR SHAFT		MILD STEEL EN1A		1		CAR-02					
	16	SKF 6000-2Z		BEARING - ID 10 OD 26		N/A		4		CAR-01, CAR-02					
E	17	ME2DMF_BH_03		BEARING HOUSING		MILD STEEL EN1A		2		CAR-01, CAR-02					
	18	ME2DMF_BH_03A		MODIFIED BEARING HOUSING		MILD STEEL EN1A		2		CAR-01, CAR-02					
	19	PIN-01		DOWEL PIN - \varnothing 3 X 25 LONG		N/A		8		CAR-P26					
	20	PIN-02		SPRING PIN - \varnothing 2 X 18 LONG		N/A		1		CAR-01					
F	21	BS 3673-4-S010M		EXTERNAL CIRCLIP - ID 10		N/A		4		CAR-01, CAR-02					
	22	BLT-01		BOLT - M4 X 40 LONG		N/A		4		CAR-P26					
	23	WSR-01		WASHER - M4		N/A		22		CAR-P26, CAR-01, CAR-02					
	24	WSR-02		WASHER - M3		N/A		2		CAR-01					
G	25	WSR-03		WASHER - M6		N/A		2		CAR-01					
	26	WSR-04		WASHER - M12		N/A		1		CAR-02					
	27	NUT-01		NUT - M4		N/A		4		CAR-P26					
	28	NUT-02		NUT - M6		N/A		2		CAR-01					
H	29	NUT-03		NUT - M12		N/A		1		CAR-02					
	30	SCW-01		SCREW - M4 X 25 LONG		N/A		8		CAR-P26					
	31	SCW-02		SCREW - M3 X 6 LONG		N/A		2		CAR-P26, CAR-01					
	32	SCW-03		SCREW - M4 X 12 LONG		N/A		6		CAR-01, CAR-02					
I	33	SCW-04		SET SCREW - M4 X 12 LONG		N/A		1		CAR-03					
	REAR SHAFT (CAR-02) AND MOTOR (CAR-03) SUBASSEMBLIES ARE EXCLUDED FROM THE TECHNICAL REALISATION SECTION.														
	<div><div><div><div>TOLERANCES</div><div>X = \pm 0.5</div><div>X.X = \pm 0.1</div><div>X.XX = \pm 0.02</div></div><div><div>ANGULAR \pm1°</div><div>SURFACE FINISH</div><div>MACHINED FACES</div><div>Ra 6.3</div></div></div><div><div>THIRD ANGLE PROJECTION</div><div></div></div><div><div>MATERIAL:</div><div>N/A</div><div>ALL DIMENSIONS ARE IN MILLIMETRES</div></div><div><div>TITLE:</div><div>BILL OF MATERIALS</div><div>DWG No.</div><div>N/A</div></div><div><div>Imperial College</div><div>London</div><div>Department of Mechanical Engineering</div><div>SHEET 1 OF 1</div><div>REVISION 4</div></div></div>														

Proposal for Manufacture

Our team has chosen to adapt our design to produce environmentally responsible toy cars for a client. The requirements of the client as well as our team's desires for the toy car are summarised in the PDS in table 5.

Table 5: PDS for an Environmentally Responsible Toy Car

Category	Elements	Statement/Criteria
Operation	Size	Of dimensions similar to our existing prototype design.
	Weight	Light enough for a child to pick up easily.
Life	Service Life	Last for at least 5 years.
	Durability	Car should be able to withstand the general rough and tumble of a child's play.
	Maintenance	Maintenance-free.
Production	Quantity	Approximately 1000.
	Cost	Manufacturing should not incur excessive setup or tooling costs as the small quantity of cars will be sold at a mid-range price.
	Materials	Materials should come from sustainable sources and be recyclable at the end of the toy car's life.
	Manufacturing Processes	Amount of energy used, and waste material produced should be minimised.
Regulatory	Safety	Transmission elements should be covered. Small parts should not be easily disassembled by a child as they pose a choking hazard.
Customer	Aesthetics	Aesthetically pleasing.

Design Embodiment for Environmental Sustainability

As the core ethos of the company is environmental sustainability, our team found it prudent to define principles that would guide our design choices in order to achieve cradle-to-grave environmental sustainability at every stage of the product lifecycle (Fig 14).



Figure 14: Achieving Environmental Sustainability at All Stages of the Product Lifecycle

The first 3 stages are very much interlinked, as each affects the other two. For example, a design that distributes stress inefficiently would require a very strong material to maintain its safety factor, while the types of manufacturing processes available are effectively limited by the shape of the component and its material.

The last 2 stages are simpler, and they gave clear-cut guidelines for our team. For the toy car to have a minimal environmental footprint during usage, it should not be powered by batteries, as they contain numerous heavy metals and toxic chemicals and are often disposed of incorrectly. Furthermore, the usage of batteries requires additional electrical components, which would present the need for e-waste recycling, which is unfavourable due to its inaccessibility. Our team's desire for the car to be entirely recyclable at its end-of-life (with currently established municipal recycling policies and technologies) ruled out electrical components and many synthetic materials such as thermoset plastics.

Design Considerations

A good design concept is fundamental to an environmentally responsible toy car. Our key principle is *simplicity* as a simple design almost always requires less complex manufacturing processes which translates to cost, material and energy savings. Hence, our team sought to eliminate unnecessary components and complexities from our existing prototype design.

Firstly, as aforementioned, we removed the electrical components, and found 3 mechanical alternatives to "power" the car: a wind-up clockwork motor, a pullback motor and a friction motor.

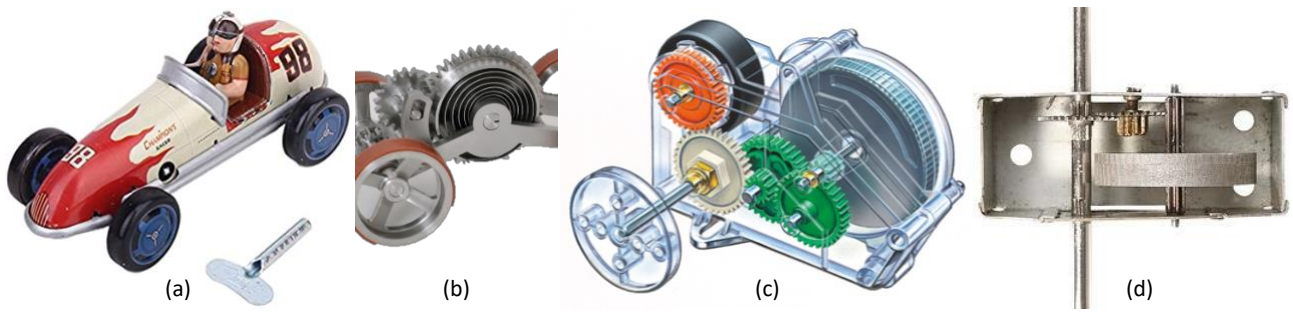


Figure 15: (a) Wind-Up Motor (b) Pullback Motor (c) Complex Friction Motor (d) Simple Friction Motor

The first 2 motors operate on the same principle of storing potential energy in a spiral torsion spring, seen in Figure 15 (b). However, both these mechanisms require a clutch or ratchet mechanism to disengage the motor once the spring has fully unwound or the car would come to an abrupt stop. These mechanisms are complex and require intricate components. This ruled out both mechanisms as it goes against our overarching principle of simplicity.

A friction motor stores energy in a flywheel connected to the wheel axles via a low gear ratio. This means that while a friction motor can be complex if it involves multiple stages of gear reduction, it can also be made extremely simple with just a single or double reduction. We chose the simplest form of a friction motor - a single reduction stage.

Secondly, given that the bulky motor and battery holder were no longer present, the chassis could be reshaped to be nearly twice as compact and simpler to manufacture (Fig 16). Additionally, it was designed to tessellate, so the same sheet of stock material could be used to manufacture the top plate with almost no wastage given an appropriate manufacturing process.

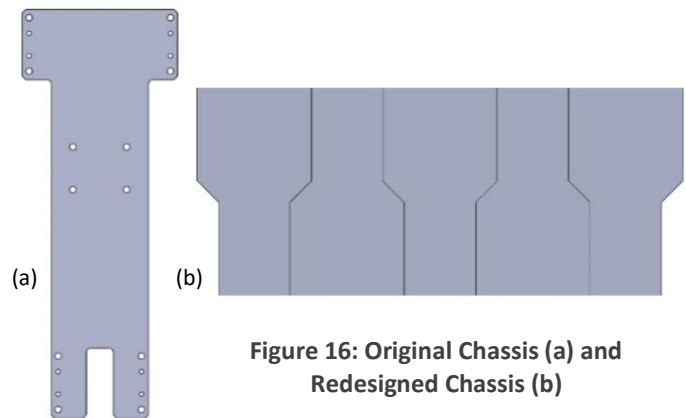


Figure 16: Original Chassis (a) and Redesigned Chassis (b)

Thirdly, the ball bearings were all replaced with simple flanged bushings. No recreational toy cars for children with dimensions similar to our design use ball bearings. We deemed ball bearings to be superfluous and unnecessary for this application and difficult for the typical household consumer to recycle at the end of the car's life.

Next, we attempted to eliminate majority of the metal fasteners. For example, fitting the wheels on the axle with an interference fit eliminates the nuts and washers used to hold it in place. Reducing the number of metal fasteners means cutting the environmental footprint associated with the production and transport of these metal fasteners from the suppliers to our manufacturing plant.

Lastly, to minimise the different types of materials used in the production of the car, our team removed the 3D printed cover and incorporated a safe, enclosed design into our chassis to cover the transmission elements.

With these design changes, we could visualise the modified prototype shown in Figure 17. This initial design is subject to further alterations after material and manufacturing process decisions.

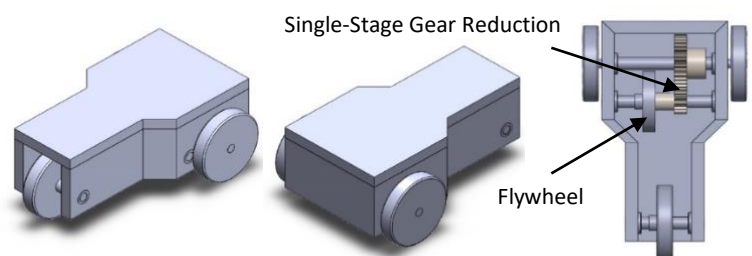


Figure 17: Initial Embodiment Design for an Environmentally Responsible Toy Car

Materials Selection

For a material to have a low environmental footprint, it needs to come from a sustainable source and be recyclable. Sustainability means that the material is sourced in a way that does not lead to the long-term decline of resources. Additionally, the material should have a low CO₂ footprint associated with its production. The CO₂ footprint is the

CO₂-equivalent mass of greenhouse gases produced and released into the atmosphere as a consequence of the production of 1 kg of the material in a form that is usable and ready for manufacture.

To narrow down our options, our team created an Ashby plot (Fig 18) from a database of materials (GRANTA EduPack, 2020). Firstly, we applied some filters to sieve out materials that were clearly unsuitable for the toy car such as glasses and ceramics. We also filtered out thermoset plastics as they are largely non-recyclable (Callister & Rethwisch, 2010). Additionally, we filtered out materials that consisted of more than 5% (by weight) materials listed in the EU or US critical raw materials list. After ranking and plotting the materials, we noted that natural materials as indicated by the green plots were congregated at the bottom left corner of the plot. This meant that they were both environmentally friendly with their low CO₂ footprint as well as favourable for our small quantity of toy cars to be sold at a mid-range price.

Following further investigation into the individual materials, our team found that nearly all these natural materials were wood-based materials. We also noted that there were some seemingly attractive options at the far-left corner of the Ashby plot within the composites “bubble” but these were particle boards which are made from wood chips binded with synthetic resins or other binders, rendering them unrecyclable. We thus looked into the natural woods. Using wood for the chassis of the car was ideal as the aesthetics would fit well with the theme of environmental responsibility. Moreover, there are various forms of wood joints (Hitchcock & King, 2020) where wooden pieces are joined geometrically without the use of metal fasteners or adhesives. An example is shown in Figure 19. This will be expounded upon further in the next section.

Having decided upon using natural woods, Table 6 was constructed comparing various material properties of the most sustainable wood types (Kolic, 2021). The wood needed to be strong yet light and inexpensive, therefore we examined their strengths, density, and price. Another relevant ranking factor is the growth rate, as the faster the wood regrows, the more renewable the material. Considering all these factors, the materials were ranked.

Table 6: Materials Selection (GRANTA EduPack, 2020)

Material	Tensile strength (MPa)	Density (kg m⁻³)	Growth rate (metre/year)	Price (GBP/m³)	Overall Rank
<i>Bamboo</i>	160 – 320	600 – 800	Up to 332	627 – 1260	1
<i>Maple</i>	61.8 – 75.5	480 - 590	0.3 – 1.1	502 - 928	2
<i>Pine</i>	92.3 - 113	760 – 920	0.3 – 0.6	796 - 1440	3
<i>White Ash</i>	86.6 – 106	600 – 740	0.3 – 0.6	944 – 1540	4
<i>Oak</i>	133 - 162	850 - 1030	0.5	4450 - 8660	5

Our team decided to choose bamboo plywood to form the chassis of the car primarily due to its fast growth rate. Bamboo is one of the fastest growing plants in the world (INBAR, 2021), reaching maturity within 4 – 7 years as compared to 25 years for softwoods and 100 years for hardwoods (Deign C, 2021). Their fast-growing nature means that they are highly renewable if sustainably sourced. Furthermore, bamboo has a high strength-to-weight ratio. In fact, it has a strength comparable to hardwoods such as oak or maple (Kaminski et al., 2016). This makes it favourable for a durable yet lightweight toy car for children.

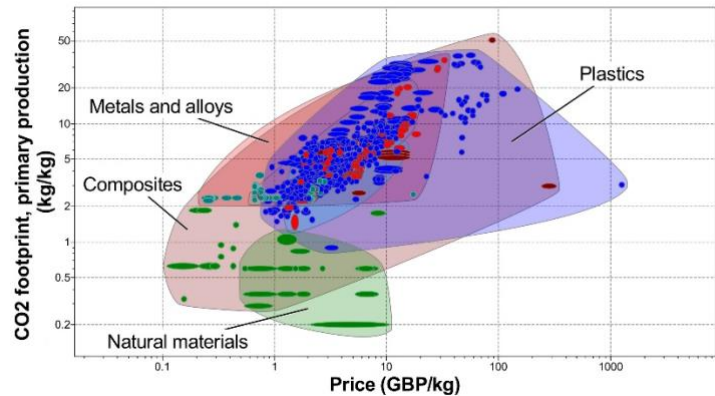


Figure 18: Ashby Plot of CO₂ Footprint Against Price (GRANTA EduPack, 2020)

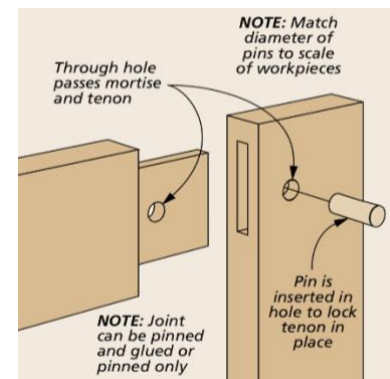


Figure 19: Mortise and Tenon Joint (Raife, 2021)

Like other forms of timber, bamboo is naturally renewable, but it needs to be sustainably sourced. There is currently no Forest Stewardship Council (FSC) certification for bamboo which can help to verify that the wood comes from well-managed forests or plantations and/or recycled sources. Therefore, during the procurement of the bamboo plywood, it is important to research and ensure that the growth and harvest of the bamboo is done responsibly. Another downside is that bamboo is mainly grown in tropical to warm temperate regions in Asia, Africa, and Central and South America. Thus, depending on the location of the manufacturing plant and the intended consumer base, the CO₂ footprint associated with the transport of bamboo might outweigh its benefits. In this case, it might be more prudent to use other locally sourced timber that also grow relatively quickly. A possible alternative would be FSC-certified pine wood.

For the shafts, our team looked at 3 classes of materials – woods, metals and plastics. For wood, we were concerned that the constant contact between moving and stationary surfaces would lead to excessive wear and splintering on a wooden shaft, which would be detrimental for the safety and durability of the toy car. The CO₂ footprint for metals and plastics are of similar orders of magnitude (Fig 18) so we considered their environmental footprint in terms of recyclability. Metals can be recycled infinitely without degradation while recycled plastics tend to require the addition of virgin material. Moreover, the recycling rates for metals are far higher than plastics due to their commercial value. For example, in 2017, the UK recycling rate for metals was 71.1% while that for plastics was 46.2% (Department for Environment, Food & Rural Affairs, 2020). Furthermore, as the perception of the public towards plastics is not favourable with at least 7 in 8 adults being fairly to very concerned about the problem of plastic waste (Ipsos, 2018), it would not be logical for a car to contain three plastic shafts when it is advertised as being environmentally responsible. We decided to use recycled aluminium as it is one of the most commonly recycled metals and requires 95% less energy to produce compared to extracting the raw metal from the ore.

Manufacturing Process

For a manufacturing process to have a low environmental footprint, it should not be energy or resource-intensive and should result in little waste materials. Therefore, of the 4 main types of manufacturing processes – casting/moulding, machining, joining, and forming – casting/moulding is generally not preferred as it involves a significant amount of heat energy.

For the wooden chassis (Fig 20), machining would be the appropriate type of manufacturing process. Normally, if we were cutting just 1 top plate from a plank of wood, an ordinary jigsaw or a band saw would be sufficient to remove the surrounding material. However, as mentioned previously, our team wanted a process that could cut the profile and its corners from a long plank of wood (Fig 16 (b)) in order to minimise wastage of material. This meant that we could not just cut off slabs of wood as the top plates were adjacent to one another.

We considered two possible options – water jet cutting or using a router with a straight bit. Water jet cutting is clean and fast with a cutting speed of 0.05 – 0.5 m s⁻¹. However, the machine's pump needs approximately 30 kW of power to pump about 7 litres of water per minute (GRANTA Edupack, 2020). Given that water conservation is an important part of environmental responsibility, our team decided to use a router. A typical ½" router uses up to 2.2 kW of power (Screwfix, 2021), much less than a water jet cutter. A router also typically costs less than £1000 (Screwfix, 2021), which is less than the capital costs of £1440 – 8620 for a water jet cutter (GRANTA Edupack, 2020). An added advantage is the versatility of the router, where different bits can be swapped out for different purposes. For 1000 cars, there is no requirement for CNC and the router can be employed manually. The side of the car measures about 150 mm in length. If we assume a feed rate of 18" min⁻¹ or 457 mm min⁻¹ (Design & Manufacturing Laboratory - UF MAE, 2021) and we make a simplified assumption that 999 cuts are needed on an extremely long plank of wood to make 1000 top plates, it would take only 5.5 man-hours of continuous cutting to manufacture this component. Nevertheless, using a CNC router on a production line is always an option if the production quantity is to be scaled up.

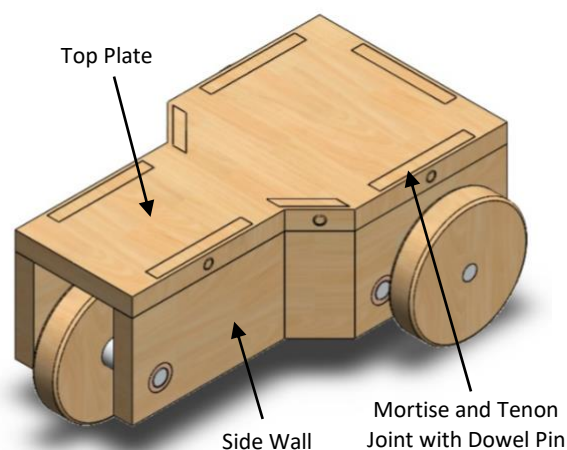


Figure 20: Wooden Chassis

The side walls have very simple geometry and can be manufactured using any type of saw although a mitre saw is recommended due to angled cuts being needed. Note that the side walls must be cut slightly taller to cater for the tenon which will be subsequently be manufactured. The chassis is deliberately designed with 45° angles as most mitre saws normally come with pre-sets for popular angles such as 45° (Toolstop, 2021). This makes it convenient and simple to make the necessary 45° bevel cuts on the side walls (Fig 21).

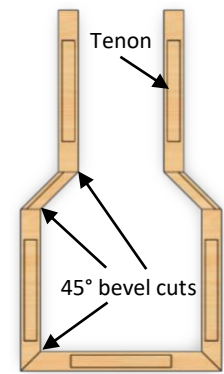


Figure 21: Top View of Side Walls

After the chassis is cut to shape, the mortise and tenon joints can be created either manually or with a dedicated tenoning machine. If the manual route is chosen, the router can once again be used with a straight bit to hollow out the mortise and to remove material around the tenon. This will incur no extra capital costs as compared to a specialised tenoning machine which typically costs a few thousand GBP (TWS Wood Machinery, 2021). Given the relatively small quantity of cars and the aim of not unnecessarily procuring tools or machines for our environmentally responsible car, it is recommended to manually create the mortise and tenon joint. Following this, the holes to mount the various components can simply be drilled using a mill for accurate positioning. A wood drill bit will be necessary to drill clean holes. Finally, the dowel pins will be manufactured on a lathe.

Similar to the original HammerHead prototype, the shaft made of recycled aluminium will still be manufactured by turning on a lathe. Since this process does not involve heat, it is deemed to be energy efficient. Finally, specialised components, such as gears and bush bearings will still be sourced from bulk suppliers, as procuring machinery to manufacture them independently would be economically and environmentally inefficient. To minimise the CO₂ footprint associated with the transport of these components to our manufacturing plant, it is advisable to source these parts from local suppliers if available.

As can be seen, the simple design of our environmentally responsible car enabled our team to utilise straight-forward, energy-efficient machining processes to manufacture our car. Consequently, the capital costs are also relatively low. If we assume that our manufacturing plant is already equipped with common equipment such as a milling machine and a lathe, our team effectively only needs to spend about £1000 on a router and £500 on a mitre saw, which translates to £1.50 per car. There are no part-specific tools such as moulds or dies so all tools used are generic and reusable for other applications.

Conclusion

As of the time of writing, the components for the HammerHead are being manufactured and nearing completion. Our team is particularly pleased with its overall design from an engineering and aesthetic standpoint. Its aggressive, sleek and striking appearance resembles the eponymous HammerHead shark, and we look forward to seeing it perform on the day of the race.

The final prototype of the HammerHead measures 514 x 198 x 73mm and weighs 1.8 kg. It is a 3-wheel, front-wheel drive car, powered by a 7 W brushed DC motor that drives the main shaft via an 11:1 reduction gearbox and a 1:3 bevel gear transmission. It is predicted to complete the race in 6.99 s with a top speed of 5.24 m s⁻¹.

The HammerHead is expected to fulfil all task requirements. It had an estimated manufacturing time of 6.7 h and an estimated cost of £587.46, well within the 12 h and £600 limits. It is easy to operate with a switch that is accessible when the car is on the floor. Having performed the stress analysis for all critical components, our team is confident that it can withstand the average person accidentally exerting their full bodyweight onto it and that it can operate for a minimum of 100 hours.

When re-designing the HammerHead as an environmentally responsible toy car, our team strived to minimise the resources and energy that were needed to manufacture the car. We simplified the design and eliminated unnecessary components and fasteners. Bamboo plywood and recycled aluminium were chosen as the primary materials for the car. The entire car is manufactured with cost-effective machining processes and tools that can be reused for other applications.

In designing the HammerHead, our team encountered various challenges requiring our critical thinking and collaborative skills. Throughout the design phase, we continuously adapted and refined the design, making decisions underpinned by engineering principles. Although the prototype has yet to be assembled, all our

calculations point towards the HammerHead fulfilling every design specification. Despite our rather unconventional design with the transmission elements mounted upside-down, we believe that choices like these allowed for the lightest and most compact design possible. Hence, we believe that the HammerHead is well set to *nail* this challenge.

References

- BBC News. 2021. *British Feet Are 'Getting Bigger And Wider'*. [online] Available at: <<https://www.bbc.co.uk/news/health-27662088>> [Accessed 13 January 2021].
- Callister, W. and Rethwisch, D., 2010. *Materials Science And Engineering: An Introduction*. 10th ed. p.536.
- Childs, P., 2019. *Mechanical Design Engineering Handbook*. 2nd ed. Oxford, United Kingdom.
- Deign, C., 2021. *Softwood Vs Hardwood*. [online] Charltonandjenrick.co.uk. Available at: <<https://www.charltonandjenrick.co.uk/news/2019/05/softwood-vs-hardwood/>> [Accessed 18 January 2021].
- Garden, H., HowStuffWorks, Garden, Improvement, DIY and Flooring, 2021. *5 Sustainable Hardwoods*. [online] HowStuffWorks. Available at: <<https://home.howstuffworks.com/home-improvement/home-diy/flooring/5-sustainable-hardwoods.htm>> [Accessed 18 January 2021].
- Gosling, G. & Kutlay, A., 2019. ME1 DMF Notes.
- Hitchcock & King. 2021. *The 6 Most Common Types Of Wood Joints | Hitchcock & King*. [online] Available at: <<https://www.hitchcockandking.co.uk/advice/the-6-most-common-types-of-wood-joints/>> [Accessed 18 January 2021].
- INBAR. 2021. *Why Bamboo & Rattan?- INBAR*. [online] Available at: <<https://www.inbar.int/why-bamboo-rattan/>> [Accessed 18 January 2021].
- Ipsos MORI. 2021. *Public Concern About Plastic And Packaging Waste Is Not Backed Up By Willingness To Act*. [online] Available at: <<https://www.ipsos.com/ipsos-mori/en-uk/public-concern-about-plastic-and-packaging-waste-not-backed-willingness-act>> [Accessed 17 January 2021].
- Kvsteel.co.uk. 2021. *EN1A Steel*. [online] Available at: <<https://kvsteel.co.uk/steel/EN1A.html>> [Accessed 15 January 2021].
- London School of Hygiene & Tropical Medicine, 2021. *The Weight Of Nations | LSHTM*. [online]. Available at: <https://www.lshtm.ac.uk/newsevents/news/2012/tacking_population_weight_crucial_for_food%20security.html> [Accessed 20 January 2021].
- n.d. *Drilling Speeds And Feeds*. [ebook] University of Florida, p.1. Available at: <<https://mae.ufl.edu/designlab/Lab%20Assignments/EML2322L-Drilling%20and%20Milling%20Speeds%20and%20Feeds.pdf>> [Accessed 18 January 2021].
- Qtcgears.com. 2021. *Spur Gears: Technical Information*. [online] Available at: <<https://qtcgears.com/tools/info/infospur.php>> [Accessed 15 January 2021].
- Raife, T., 2021. *Pinned Mortise & Tenon Joinery*. [online] Woodsmith. Available at: <<https://www.woodsmith.com/article/pinned-mortise-tenon-joinery/>> [Accessed 18 January 2021].
- Shigley, J., Mischke, C., Budynas, R. and Shigley, J., 2006. *Shigley's Mechanical Engineering Design*. New York: McGraw-Hill Higher Education, p.32.
- S, K., A, L. and D, T., 2016. Structural use of bamboo. Part 1: Introduction to bamboo. *The Institution of Structural Engineers*, [online] p.3. Available at: <[https://www.istructe.org/journal/volumes/volume-94-\(2016\)/issue-8/structural-use-of-bamboo-part-1-introduction-to-b/](https://www.istructe.org/journal/volumes/volume-94-(2016)/issue-8/structural-use-of-bamboo-part-1-introduction-to-b/)> [Accessed 18 January 2021].
- Skf.com. 2011. [online] Available at: <[https://www.skf.com/binaries/pub12/Images/0901d1968013be94-SKF-bearing-maintenance-handbook---10001_1-EN\(1\)_tcm_12-463040.pdf](https://www.skf.com/binaries/pub12/Images/0901d1968013be94-SKF-bearing-maintenance-handbook---10001_1-EN(1)_tcm_12-463040.pdf)> [Accessed 11 January 2021].
- Toolstop. 2021. *Mitre Saw Buying Guide*. [online] Available at: <<https://www.toolstop.co.uk/blog/buying-guides/mitre-saw-buying-guide>> [Accessed 19 January 2021].
- TWS Wood. 2021. *Tenoning Machines - Tenoner Machine For Sale | TWS Wood*. [online] Available at: <<https://www.twswood.co.uk/machinery/tenoners-woodworking-machinery/>> [Accessed 19 January 2021].
- Van Aken, D., 2001. Relationship Between Hardness and Strength. [online] p.6. Available at: <https://scholarsmine.mst.edu/matsci_eng_facwork/1402/> [Accessed 13 January 2021].
2020. *GRANTA Edupack*. Ansys.
2020. *UK Statistics On Waste*. [ebook] London: Department for Environment Food & Rural Affairs, p.4. Available at: <https://assets.publishing.service.gov.uk/government/uploads/system/uploads/attachment_data/file/918270/UK_Statistics_on_Waste_statistical_notice_March_2020_accessible_FINAL_updated_size_12.pdf> [Accessed 19 January 2021].
2021. [image] Available at: <<https://www.amazon.co.uk/MagiDeal-Wind-Up-Retro-Racing-Collectible/dp/B01B7HVHCO>> [Accessed 12 January 2021].
2021. [image] Available at: <<https://www.wired.com/2011/04/its-a-wind-up-gorgeous-spring-powered-toy-car-not-for-kids/>> [Accessed 12 January 2021].
2021. [image] Available at: <<https://www.tamiya.com/english/products/70222/index.htm>> [Accessed 12 January 2021].
2021. [image] Available at: <<https://www.betterequipped.co.uk/friction-motor-4825>> [Accessed 12 January 2021].
2021. [online] Available at: <<https://www.screwfix.com/c/tools/routers/cat830904>> [Accessed 19 January 2021].

Appendices

Appendix A: Derivation of Ideal Gear Ratio

The orange line in Figure 22 shows the torque-speed characteristic curve of the supplied motor excluding the 11:1 reduction gearbox. As can be seen, torque τ is not a constant value throughout the range of operating speeds but rather, decreases linearly as speed ω increases up to the no-load speed of 569 rad s^{-1} . However, these torque values are not equivalent to the torque exerted on the main shaft as the torque is amplified or reduced depending on the gear ratio, while the speed experiences the opposite effect.

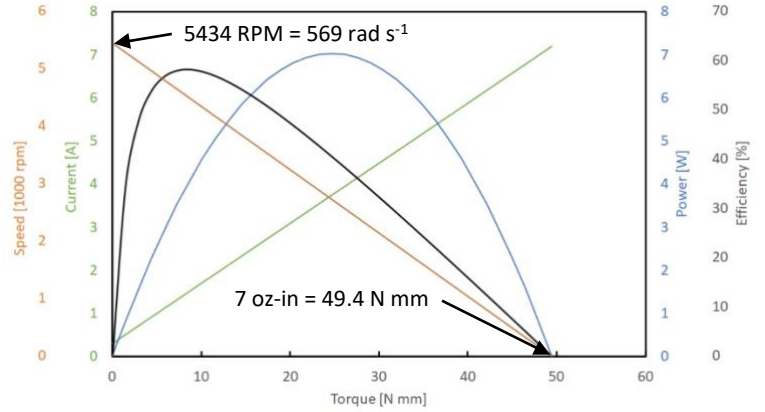


Figure 22: Motor Characteristic Curves

The gear ratio GR is defined as:

$$GR = \frac{\omega_{Driven\ Gear}}{\omega_{Driving\ Gear}} = \frac{No.\ of\ Teeth_{Driving\ Gear}}{No.\ of\ Teeth_{Driven\ Gear}} = \frac{No.\ of\ Teeth_{Reduction\ Gearbox\ Output\ Shaft\ Bevel\ Gear}}{No.\ of\ Teeth_{Main\ Shaft\ Bevel\ Gear}} \quad (1)$$

Equations 2 and 3 show how the 11:1 reduction gearbox and the gear ratio of our bevel gears alter the stall torque T and no-load speed Ω of the *main shaft* respectively.

$$T = 0.0494 \times 11 \times GR \quad (2)$$

$$\Omega = 569 \div 11 \div GR \quad (3)$$

Hence, the equation of the torque-speed characteristic curve of the *main shaft* is:

$$\tau = -\frac{T}{\Omega}(\omega) + T \quad (4)$$

It is worth emphasising that T and Ω are constants while τ and ω are variables which now refer to the torque and speed of the main shaft and not the motor in the above equation. They will refer to these for all subsequent equations. We note that the speed of the main shaft is the speed at which the wheels are rotating. For wheels of radius r which rotate without slipping, the linear velocity of the car v is given by:

$$v = r\omega \Rightarrow \omega = \frac{v}{r} \quad (5)$$

$$\therefore \tau = -\frac{Tv}{\Omega r} + T \quad (6)$$

The force F_t that the driven front wheels exert on the ground to propel the car forward comes from the torque of the main shaft and is given by:

$$F_t = \frac{\tau}{r} \quad (7)$$

However, we note that there will always be drivetrain power losses from the gears and bearings. Hence, we multiply F_t by an efficiency factor η . The efficiency of a ball bearing is 98% while the efficiency of spur gears and bevel gears are 98% and 95% respectively (Childs, 2019). Our car consists of 4 ball bearings, 2 sets of 2 meshing spur gears within the 11:1 reduction gearbox and a single set of 2 meshing bevel gears. Hence, η is taken to be:

$$\eta = (0.98 \times 4) \times (0.98 \times 2) \times (0.95 \times 1) = 84.2\% \quad (8)$$

Besides the drivetrain power losses, there are also external resistive forces F_r on the car such as friction. Newton's second law for a car of mass m (Fig 23) thus gives:

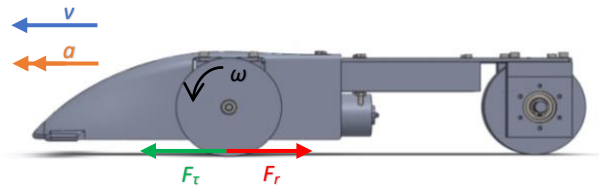


Figure 23: Kinematic diagram with horizontal forces

$$m \frac{dv}{dt} = \eta F_r - F_r = \eta \left(\frac{\tau}{r} \right) - F_r = \eta \left(-\frac{Tv}{\Omega r} + T \right) \left(\frac{1}{r} \right) - F_r$$

$$\Rightarrow \frac{dv}{dt} = -\frac{\eta T}{m \Omega r^2} v + \frac{\eta T}{mr} - \frac{F_r}{m} \quad (9)$$

Equation 9 is a first-order linear differential equation that can be solved via the separation of variables method or the usage of an integrating factor. Either way, we obtain velocity v of the car as a function of time t :

$$v = \left(\frac{\eta T}{r} - F_r \right) \left(\frac{\Omega r^2}{\eta T} \right) \left(1 - \exp \left(\frac{-\eta T}{m \Omega r^2} t \right) \right) \quad (10)$$

Acceleration a can be found by differentiating Equation 10 again while distance s can be obtained by integrating Equation 10 and applying the boundary condition of $s = 0$ when $t = 0$.

$$s = \int v dt = \left(\frac{\eta T}{r} - F_r \right) \left(\frac{\Omega r^2}{\eta T} \right) \left(t + \frac{m \Omega r^2}{\eta T} \exp \left(\frac{-\eta T}{m \Omega r^2} t \right) - \frac{m \Omega r^2}{\eta T} \right) \quad (11)$$

$$a = \frac{dv}{dt} = \left(\frac{\eta T}{r} - F_r \right) \left(\frac{1}{m} \right) \exp \left(\frac{-\eta T}{m \Omega r^2} t \right) \quad (12)$$

These functions can be plotted using a Python code.

Appendix B: Mass Estimation

Table 7 was used to derive the total weight of the HammerHead.

Table 7: Mass estimation calculations.

Part	Mass (g)	Explanation
Main Shaft	130	Density of Mild Steel EN1A: 7.85 g cm^{-3} Volume of original shaft: $\pi \times 0.7^2 \times 9 + \pi \times 0.5^2 \times (2.2 + 1.6) + 2 \times \pi \times 0.3^2 \times 3.6 = 18.87 \text{ cm}^3$ Mass of original given shaft: $7.85 \times 18.87 = 148 \text{ g}$ Estimated mass removed: 20 g Final estimated mass of main shaft: 130 g
Rear Shaft	100	Density of Mild Steel EN1A: 7.85 g cm^{-3} Volume of shaft: $\pi \times 0.7^2 \times 9 + \pi \times 0.5^2 \times (2.2 + 1.6) = 16.84 \text{ cm}^3$ Mass of original given shaft: $7.85 \times 16.84 = 132 \text{ g}$ Estimated mass removed: 32 g Final estimated mass of main shaft: 100 g
Cover	105	Density of ABS plastic: 1.05 g cm^{-3} Estimated volume of our cover: 100 cm^3 Estimated mass of cover: $1.05 \times 100 = 105 \text{ g}$
Chassis	162	Density of Aluminum 6082 T6: 2.7 g cm^{-3} Estimated volume of cover: 60 cm^3 Estimated mass of cover: $2.7 \times 60 = 162 \text{ g}$
Gear	40	Estimated based on mass of sets of bevel gears with gear ratio 1:3
Bearings	60	Estimated mass of one bearing with ID 10 and OD 26: 15 g Mass of four bearings: $15 \times 4 = 60 \text{ g}$
Bearing housing	628	Density of Mild Steel EN1A: 7.85 g cm^{-3} Calculated volume of one bearing housing: 20 cm^3 Mass of one bearing housing: $7.85 \times 20 = 157 \text{ g}$ Mass of four bearing housing: $157 \times 4 = 628 \text{ g}$
3 Wheels	270	Density of Silicone Rubber 60A Shore Hardness: 1.20 g cm^{-3} Volume of two front wheel (ID 6 mm, OD 80 mm, thickness 15 mm): $2 \times 75.0 = 150 \text{ cm}^3$ Volume of one rear wheel (ID 12 mm, OD 80 mm, thickness 15 mm): 73.7 cm^3 Mass of all wheel: $1.20 \times (150 + 73.7) = 270$
Switch	5	Estimated
Motor with gear box	238	Given in brief
Battery holder	10	Estimated
Batteries	50	Estimated mass of 3 alkaline AA batteries.
TOTAL	1798 g \approx 1.8 kg	

Appendix C: Bevel Gear Calculations

Straight bevel gears are recommended for pitch line velocities ranging from 0 to 5 m s⁻¹ (Childs, 2019). From Equation 13, the pitch line velocity V of our gears was calculated to be 1.474 m s⁻¹. Straight bevel gears are therefore appropriate and there is no requirement for spiral bevel gears.

$$V = \omega \frac{PCD}{2} = \frac{v_{car}}{r_{wheel}} \frac{PCD}{2} = \frac{5.24}{0.04} \times \frac{0.0225}{2} = 1.474 \text{ m s}^{-1} \quad (13)$$

The two primary failure modes for gears are tooth breakage from excessive bending stress, and surface pitting or wear from excessive contact stress. The ANSI/AGMA 2003-B97 standard enables us to estimate the safety factors SF for these two failure modes (Childs, 2019). We note that there are numerous factors in Equations 14 to 17. For factors which we deemed to be negligible or those which we had insufficient or inconclusive data for, we took their values to be unity, meaning that they had no effect on the stresses.

$$\text{Bending Stress } \sigma_F = \frac{2000T_{q1}}{Fd_{e1}} \frac{K_A K_v Y_x K_{H\beta}}{m_{et} Y_\beta Y_J} = 3.54 \text{ MPa} \quad (14)$$

Symbol	Definition	Value
T_{q1}	Operating pinion torque (N m)	0.1811 N m
K_A	Overload factor	1.00 (Uniform prime mover and driven machine characteristics)
K_v	Dynamic factor	NA (Insufficient knowledge of transmission accuracy number)
Y_x	Size factor	0.5 ($m_{et} < 1.6$)
$K_{H\beta}$	Load distribution factor	1.1 (1 straddle mounted gear and 1 non straddle mounted gear)
F	Net face width (mm)	7.10 mm
d_{e1}	Pinion outer pitch diameter (mm)	22.50 mm
m_{et}	Outer traverse module (mm)	1.5 mm
Y_β	Tooth lengthwise curvature factor	1 (Straight bevel gears)
Y_J	Bending strength geometry factor	0.235

$$\text{Permissible Bending Stress } \sigma_{FP} = \frac{\sigma_{Flim} Y_{NT}}{S_F K_\theta Y_Z} = 24.0 \text{ MPa} \quad (15)$$

Symbol	Definition	Value
σ_{Flim}	Allowable bending stress (MPa)	23.8 MPa (Approximated with fatigue strength (GRANTA Edupack, 2020))
Y_{NT}	Stress cycle factor	$1.6831(7.51 \times 10^6)^{-0.0323} = 1.009$ ($3 \times 10^6 \leq \text{Number of cycles} \leq 10^{10}$ for general conditions)
S_F	Bending safety factor	1 (For maximum permissible stress)
K_θ	Temperature factor	1 (Normal conditions)
Y_Z	Reliability factor	1 (Fewer than 1 failure in 100)

$$\text{Contact Stress } \sigma_H = Z_E \sqrt{\frac{2000T_{q1}}{Fd_{e1}^2 Z_I} K_A K_v K_{H\beta} Z_x Z_{xc}} = 20.4 \text{ MPa} \quad (16)$$

Symbol	Definition	Value
Z_E	Elastic coefficient (MPa ^{0.5})	$\left(2\pi(1-\nu^2/E)\right)^{-0.5} = 24.15$ (Poisson's ratio $\nu = 0.34$, Young's modulus $E = 3240$ MPa (GRANTA Edupack, 2020))
T_{q1}	Operating pinion torque (N m)	0.1811 N m
K_A	Overload factor	1.00 (Uniform prime mover and driven machine characteristics)
K_v	Dynamic factor	NA (Insufficient knowledge of transmission accuracy number)
$K_{H\beta}$	Load distribution factor	1.1 (1 straddle mounted gear and 1 non straddle mounted gear)
Z_x	Size factor	0.5 ($F < 12.7$ mm)
Z_{xc}	Crowning factor	NA (Insufficient information on teeth crowning)
F	Net face width (mm)	7.10 mm

d_{e1}	Pinion outer pitch diameter (mm)	22.50 mm
Z_I	Pitting resistance geometry factor	0.0775

$$\text{Permissible Contact Stress } \sigma_{HP} = \frac{\sigma_{Hlim} Z_{NT} Z_W}{S_H K_\theta Z_Z} = 87.2 \text{ MPa} \quad (17)$$

Symbol	Definition	Value
σ_{Hlim}	Allowable contact stress	64.9 MPa (Approximated with yield strength (GRANTA Edupack, 2020))
Z_{NT}	Stress cycle factor	$3.4822(7.51 \times 10^6)^{-0.0602} = 1.343$ ($10^4 \leq \text{Number of cycles} \leq 10^{10}$)
Z_W	Hardness ratio factor	NA (No difference in hardness between the 2 gears)
S_H	Contact safety factor	1 (For maximum permissible contact stress)
K_θ	Temperature factor	1 (Normal conditions)
Z_Z	Reliability factor	1 (Fewer than 1 failure in 100)

Appendix D: Bearing Calculations

The HammerHead is predicted to reach a top speed of 5.24 m s^{-1} , resulting in a maximum angular speed of 20.85 rev s^{-1} for the shaft. Using this angular speed, the L_{10} basic life rating for 100 hours was calculated:

$$L_{10} = 20.85 \times 100 \times 60 \times 60 = 7.51 \times 10^6 \quad (18)$$

Using the L_{10} value, the minimum dynamic load rating C_{min} can then be calculated:

$$C_{min} \geq F \times (L_{10})^{\frac{1}{k}} \quad (19)$$

The constant $k = 3$ for ball bearings (Childs, 2019). For a combination of radial and axial loads – F_r and F_a , the equivalent radial load F is given by:

$$F = XF_r + YF_a \quad (20)$$

where X and Y are the radial and axial load factors to be looked up in the table of factors given in the supplier's catalogue. The radial load on the bearings on the main shaft is a combination of the load from the car's weight and the radial load from the bevel gear. The axial load on the bearings is solely from the axial load imposed by the bevel gear. To be conservative, we assume the main shaft to bear the entire weight of the car. Therefore, a bearing on the main shaft bears half the car's weight:

$$F_w = 0.5mg = 0.5 \times 1.8 \times 9.81 = 8.829 \text{ N} \quad (21)$$

The radial and axial forces from the bevel gear can be calculated with these equations (Childs, 2019):

$$F_r = F_t \tan \varphi \cos \alpha \quad (22)$$

$$F_a = F_t \tan \varphi \sin \alpha \quad (23)$$

where F_t is the force due to the torque, φ is the pressure angle which is 20° as stated in the HPC Gears catalogue, and α is the pitch cone angle. Knowing that the maximum torque on our main shaft is the stall torque multiplied by the overall gear ratio, we can use this value and the pitch circle radius of the gear to calculate F_t :

$$F_t = \frac{T}{r} = \frac{0.0494 \times 11 \times \frac{1}{3}}{0.01125} = 16.10 \text{ N} \quad (24)$$

The pitch cone angle α was calculated using the ratio of the number of teeth in the 2 gears (Childs, 2019):

$$\alpha = 90 - \tan^{-1} \left(\frac{N_G}{N_P} \right) = 90 - \tan^{-1} \left(\frac{45}{15} \right) = 18.43^\circ \quad (25)$$

Using Equations 22 and 23, the total radial and axial loads were calculated to be 14.39 N and 1.85 N respectively. From the table of factors (Gosling, 2019), X and Y were found to be 1 and 0 respectively. Equation 21 gave an equivalent radial load of 14.39 N. Therefore, using Equation 19, the minimum dynamic load rating is 2.82 kN. The

6000-2Z bearings have a dynamic load rating of 4.75 kN. Therefore, it is very unlikely that the bearings will fail after a 100 h of operation.

Appendix E: Shaft Calculations

Main Shaft

The maximum bending moment of 6.2 N m is constant across the \varnothing 10 mm and \varnothing 12 mm sections of the main shaft. The second moment of area I for the smaller \varnothing 10 mm section is given by:

$$I = \frac{\pi r^4}{4} = \frac{\pi \times 0.005^4}{4} = 4.909 \times 10^{-10} \text{ m}^4 \quad (26)$$

The stress σ caused by the bending moment is given by:

$$\sigma = \frac{Mr}{I} = \frac{6.2 \times 0.005}{4.909 \times 10^{-10}} = 63.1 \text{ MPa} \quad (27)$$

For fatigue failure analysis, we considered an extreme scenario where the car was operated continuously for a 100 h. The main shaft experiences a torsional load from the motor and an axial load due to the bending moment from the weight of the car (Fig 24).

The shear stress τ caused by the torque T is given by:

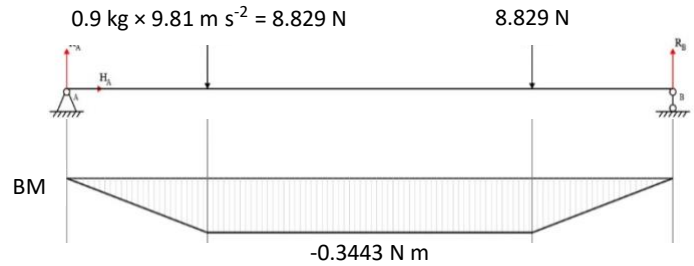


Figure 24: Bending Moment Diagram Due to Car's Weight

$$\tau = \frac{Tr}{J} = \frac{Tr}{\frac{\pi r^4}{2}} = \frac{2T}{\pi r^3} = \frac{2 \times 0.181}{\pi (0.006)^3} = 533.5 \text{ kPa} \quad (28)$$

The axial stress σ caused by the bending moment M is given by:

$$\sigma = \frac{Mr}{I} = \frac{Mr}{\frac{\pi r^4}{4}} = \frac{4M}{\pi r^3} = \frac{4 \times 0.3443}{\pi (0.006)^3} = 2.030 \text{ MPa} \quad (29)$$

We note that as the shaft rotates, an element on the surface of the shaft experiences a constant shear stress but the axial stress alternates between tension and compression in a fully reversed sinusoidal cycle. For combined uniaxial and torsional loading, the alternating and mean von Mises stress (Budynas & Nisbett, 2011) is given by:

$$\sigma' = \sqrt{\sigma^2 + 3\tau^2} \quad (30)$$

$$\sigma'_a = \sqrt{(2.030 \times 10^6)^2 + 3 \times 0^2} = 2.030 \text{ MPa} \quad (31)$$

$$\sigma'_m = \sqrt{0^2 + 3 \times (533.5 \times 10^3)^2} = 924.0 \text{ kPa} \quad (32)$$

Using the Goodman criterion (Budynas & Nisbett, 2011), we can estimate the safety factor for fatigue failure:

$$\frac{1}{SF} = \frac{\sigma'_a}{S_e} + \frac{\sigma'_m}{S_{ut}} \quad (33)$$

where S_e is the endurance limit and S_{ut} is the ultimate tensile strength. For steels, a rule of thumb for estimating the fatigue limit is one-half of the ultimate tensile strength (Van Aken, 2001). The tensile strength of EN1A steel is 240 – 400 MPa (KV Steel Services, 2021). Hence:

$$\frac{\sigma'_a}{S_e} + \frac{\sigma'_m}{S_{ut}} = \frac{2.030 \times 10^6}{0.5 \times 240 \times 10^6} + \frac{924.0 \times 10^3}{240 \times 10^6} = \frac{1}{48.2} \quad (34)$$

As this value is less than 1, the main shaft theoretically has an infinite lifespan for these loading conditions, with a safety factor of 48.2. Note that this calculation did not take into account the Marin modification factors (Budynas & Nisbett, 2011) which quantify the effects of surface condition, size, temperature and other miscellaneous factors. However, the extremely large safety factor means that such a rigorous analysis is excessive. We can therefore safely conclude that the main shaft will last for 100 h of operation.

Rear Shaft

The stress σ in the middle of the shaft caused by the maximum bending moment of 11.4 N m is given by:

$$\sigma = \frac{Mr}{I} = \frac{Mr}{\frac{\pi r^4}{4}} = \frac{4M}{\pi r^3} = \frac{4 \times 11.4}{\pi(0.006)^3} = 67.2 \text{ MPa} \quad (35)$$

Appendix F: Chassis Calculations

The top plate of the chassis has a 69.0 x 3.0 mm rectangular cross-section while the box bars have a 25.4 x 25.4 mm square perimeter and a wall thickness of 2.4 mm.

The second moment of area I for the top plate is given by:

$$I = \frac{bd^3}{12} = \frac{0.0690 \times 0.003^3}{12} = 1.553 \times 10^{-10} \text{ m}^4 \quad (36)$$

The second moment of area I for a single box bar is given by:

$$I = \frac{0.0254 \times 0.0254^3}{12} - \frac{0.0206 \times 0.0206^3}{12} = 1.968 \times 10^{-8} \text{ m}^4 \quad (37)$$

The stress at the middle of the chassis is supported by the top plate and 2 box bars beneath (Fig 25) while the stress at the rear region is supported solely by the top plate.

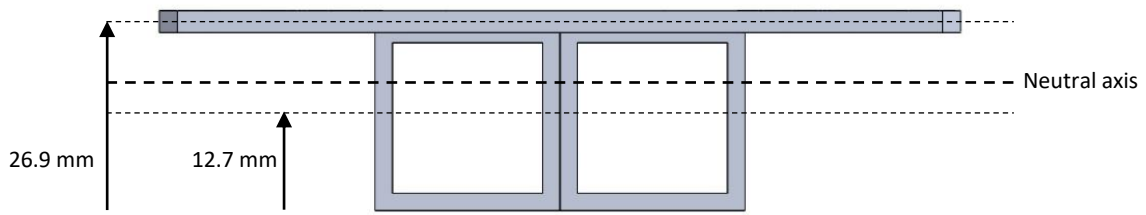


Figure 25: Chassis Cross-Section in the Middle

The neutral axis can be calculated as follows:

$$\bar{y} = \frac{(69.0 \times 3.0)(0.0269) + 2(25.4^2 - 20.6^2)(0.0127)}{(69.0 \times 3.0) + 2(25.4^2 - 20.6^2)} = 0.0172 \text{ m} \quad (38)$$

The parallel axis theorem can be used to calculate the second moment of area of this cross-section:

$$I = [1.553 \times 10^{-10} + (0.069 \times 0.003)(0.0172 - 0.0269)^2] + 2[1.968 \times 10^{-8} + (0.0254^2 - 0.0206^2)(0.0172 - 0.0127)^2] = 6.793 \times 10^{-8} \text{ m}^4 \quad (39)$$

From the bending moment diagram (Fig 12), the bending moment in the middle of the chassis is -26.00 N m while that at the rear is -7.456 N m.

The stress in the middle of the chassis is:

$$\sigma = \frac{26.00 \times 0.0172}{6.793 \times 10^{-8}} = 6.58 \text{ MPa} \quad (40)$$

The stress at the rear is:

$$\sigma = \frac{7.456 \times 0.0015}{1.553 \times 10^{-10}} = 72.0 \text{ MPa} \quad (41)$$